PROGRESS REPORT
Covering Period from 15 September 1964
to 15 March 1965

RADIATION DAMAGE TO SEMICONDUCTORS BY HIGH-ENERGY ELECTRON AND PROTON RADIATION

John C. Corelli

Sponsored by the National Aeronautics and Space Administration

under Grant NsG-290

Department of Nuclear Engineering and Science
Rensselaer Polytechnic Institute
Troy, New York

Table of Content

I. Introduction and Summary

The results presented in this report were obtained during the six month period 15 September 1964 to 15 March 1965. The following personnel were actively engaged in the research program:

Faculty:

Dr. John C. Corelli (Half time)

Adjunct Professors James W. Corbett* and George D. Watkins* and Professor H. B. Huntington of the Physics Department served as part time consultants.

Graduate Students:

Mr. John F. Becker (Left March 15, 1965)

Mr. Li-Jen Cheng

Mr. Orrin H. Merrill

Mr. Arne Kalma

Mr. John E. Fischer (AEC Fellow)

Research Technician:

James W. Westhead

Undergraduate Thesis Students (Physics Department):

Mr. Martin R. Gaerttner

Mr. Martin Weinhous

---

*Full time scientists at the General Electric Research Laboratory, Schenectady, New York.

The general topics which are reported herein are summarized briefly:

1. Carrier lifetime experiments in n-type germanium (Sb-doped) irradiated with ≈50 Mev electrons at 86°K with subsequent annealing experiments to 625°K in which recovery characteristics are examined for both short lived recombination centers $\lesssim$ 500 microseconds and long lived "trapping centers $\gtrsim$ 1000 microseconds.

2. The annealing of infrared defect absorption bands in 60 Mev electron irradiated (at 320°K) pulled and floating zone silicon. The annealing experiments were run from 340°K to 800°K.

3. Studies on the electrical properties of high resistivity germanium after 320°K irradiation with electrons of 15 - 50 Mev.

4. Low temperature ($\lesssim$ 20°K) irradiation and annealing of electrical properties of 45 Mev electron-irradiated pulled and floating zone silicon.

5. Infrared studies with 45 Mev electron-irradiated oriented single crystal silicon to study anisotropy characteristics of defects using stress techniques.

6. Initial results on the use of photoconductivity to study defects induced in silicon by 45 Mev electrons at 300°K and 80°K.

Portions of the results obtained in the research program have been given in various presentations and papers during the period 15 September 1964 to 15 March 1965 and are listed below:

1. "Carrier Lifetime Studies in Electron (10 - 55 Mev) and Proton (25 - 110 Mev) Irradiated Germanium" by J. E. Fischer and J. C. Corelli. J. Appl. Phys. 35, 3531 (1964).

2. "Recovery of 45 Mev Electron-Induced Defects in n-type Silicon from 80°K to 350°K" by Li-Jen Cheng and J. C. Corelli. Bull. Am. Phys. Soc. 9, 654 (1964).

II. Carrier Lifetime Experiments in 10 - 50 Mev Electron-Irradiated Germanium

John E. Fischer

In the last progress report[3] we mentioned that we had received a medical X-ray machine and a new X-ray triode from the General Electric Company. The power supply was modified to provide 10 nanosecond pulses of X-rays by biasing the grid at 2 KV with respect to the filament, then driving the grid slightly positive by discharging five feet of RG-8 coaxial cable with a mercury-wetted relay. The X-ray pulses obtained were extremely clean; however, the peak X-ray intensity was limited to about 10^3 R/sec by heat dissipation of the filament. This intensity was sufficient to produce an injection level $\Delta n/n$ of less than 0.3% in high-resistivity germanium. At this time a cold-cathode flash X-ray machine* was purchased, which is capable of producing 10^7 R/sec. Preliminary tests indicate that injection levels in excess of 35% are now obtainable in $\sim 10\,\Omega$-cm germanium using 50/ns pulses of 150 KVP X-rays. The use of this machine for making lifetime measurements was first suggested to us by Dr. O. L. Curtis.

A series of experiments were performed on Sb-doped germanium using the same xenon flashtube arrangement as before (see last two progress reports).[3] These will be discussed in some detail

---

*Model 845, Field Emission Corporation, McMinnville, Oregon.

since they shed light on the question of the origin of radiation-induced trapping and the difference in annealing behavior between high-energy and low-energy damage.

The first experiment of this series consisted of irradiating at 86°K a well-polished piece of 8.5Ω-cm material (¼" x ¼" x 3/4") to a flux of ≈5 x 10^{14} e/cm^2 of 45 - 55 Mev. This run was performed at the 22½° port of the NASA switcher magnet; due to temporary difficulties with the Linac, the input beam to the switcher was rather broad in energy, leading to large uncertainties in flux and energy at the sample. This dose was sufficient to increase the 86°K lifetime from 30 μsec to 10 msec in the dark, indicating an extremely strong trapping process. The cryostat was then removed from the target room and 10 minute isochronal anneals were performed in situ up to 420°K, at which point the solder melted. The annealing was carried to 652°K by re-etching and reapplying leads after each anneal, the heating being done in a silicone oil bath in a diffusion furnace.

It is known that trapping is manifested in two ways; either a long tail appears on the time decay of excess conductivity (as seen in silicon by Haynes and Hornbeck,[1] among others[4]), or the decay remains exponential and the lifetime increases with decreasing temperature.[2] The latter case applied here, no doubt, because the trap density and/or cross-section far exceeded the corresponding recombination level values at low temperatures.

It is also known that the trapping behavior can be reduced by shining light on the sample.[1, 4] This is usually interpreted

as follows: the light excites electrons from the valence band into the conduction band which are then captured by the trap (assuming an electron trap), and the trap is no longer highly attractive to xenon-light-induced electrons, which can now proceed to recombination centers and be removed from circulation. In our case we were able to reduce the lifetime from 10 msec to 1 msec (at 86°K) in this manner. We must emphasize that in all cases the decays were exponential to within a few per cent at all temperatures and throughout all the anneals.

A brief sample of the results will now be presented. In Figure 1 we plot τ vs. 1000/T before irradiation and after several anneals, the data here all being taken in the dark. The data shown were taken as the sample cooled down from each successive annealing temperature, so naturally one does not get the full picture after the earlier anneals.

The shape of the pre-irradiation curve is worthy of comment, being rather similar to that for p-type germanium, as shown in the last progress report,[3] namely, two distinct "slopes" are apparent. The high-temperature slope is $\sim$.2 ev, in agreement with observations by Curtis;[5] the low-temperature value is $<$.05 ev, as in the indium-doped germanium sample. If one assumes that recombination in unirradiated material occurs through <u>two</u> independent Shockley-Read[6] levels, the observed lifetime is given by

$$\frac{1}{\tau} = \frac{1}{\tau_1} + \frac{1}{\tau_2}$$

Now the observed pre-irradiation behavior can be explained by summing in this fashion two levels, one of which has approximately the low-temperature slope ($\sim$.05 ev) and one of which is about .05 ev deeper than the high-temperature slope. The number of parameters involved makes it prohibitive to obtain an exact fit in this case, but an example is given in Figure 2 to give an idea of what can happen. The conclusion is fairly obvious: measurements must be carried to sufficiently low temperatures to determine if there are shallow levels which lower the high-temperature slope. In the example given (in which the density of extrinsic carriers is about one-half that in the sample shown in Figure 1), the presence of two levels in the same half of the gap as the Fermi level give rise to an observed high-temperature slope of $\sim$.08 ev, whereas the two levels are 0.05 ev and 0.15 ev. The observed slope is closer to the former value because the product of hole cross-section and level density was taken as 10^2 larger than the deeper level. Referring to Figure 1, it is entirely possible that one of the observed levels before irradiation is associated with the surface (since we used unfiltered light, which creates large gradients near the illuminated surface); we hope to resolve this question with the X-ray equipment.

We return now to the problem at hand. Figure 3 represents the isochronal annealing behavior of the traps (reference temperature = 100°K) and the recombination centers (286°K). We have chosen to plot log (1 - f) for traps and log f for recombination

centers; this may pose some slight difficulty in studying the plot, but the details show up much more clearly. The fraction not annealed, f, is given by

$$f = \pm \left(\frac{1/\tau - 1/\tau_o}{1/\tau_i - 1/\tau_o} \right)$$

where τ_i, τ_o and τ denote pre-irradiation, pre-anneal and post-anneal values of lifetime at the reference temperature. The (+) sign holds for recombination centers and the (—) sign for traps. Here again, all measurements are in the dark. The values of $1/\tau_o$ for traps and $1/\tau_i$ for recombination centers are not directly known; the former was taken as zero and the latter as 10^5 sec^{-1}.

The following observations can be made, referring to Figure 3:

1. Both types of defect level persist to very high temperatures. In similar material irradiated at room temperature with γ-rays, Curtis[7] observes that f is down to 0.04 at 485°K whereas we still have $\approx$ 20% left at that temperature.

2. Two closely-spaced "stages" of trap annealing occur below room temperature, accounting for less than 0.5% of the recovery. Up to 390°K, the trap and recombination recovery are apparently uncorrelated. The first point on the recombination curve at 304°K represents the first anneal in which the lifetime showed any decrease with decreasing temperature. On the basis of one sample, the nature of the defects responsible for these two peaks cannot be speculated on. We will present evidence later which suggests that they are characteristic of high-energy bombardment.

3. Between 390°K and 480°K, about 15% of both types of levels anneal out. This suggests that they may belong to the same defect, although in other regions of annealing temperature there is no such correlation.

4. There is an <u>increase</u> of trap density of about 12% accompanying a <u>decrease</u> of recombination center density of $\sim$18% between 480°K and 600°K. This suggests just the opposite of (3), namely, some constituent of the defect which exhibits recombination behavior is being freed and is ultimately associating with some other defect to produce trapping levels. Similar behavior has been observed in silicon by Watkins and Corbett[8] using ESR, and by other members of our group[3] using infrared absorption, that is, the disappearance of one type of ESR spectrum or absorption band may be accompanied by the increase of another.

It is also observed that, for anneals below 480°K, the fractional increase in $1/\tau$ at low temperature by shining white light on the sample is roughly the same after each anneal. This is to be expected since these photo-induced carriers must travel across the band gap and then into a trap, so that a change in the trap energy with annealing temperature (which is suggested in Figure 1) should not change the number which are filled by light. On the other hand, illumination with infrared light will excite carriers from a band directly into the traps, and the wavelength used will be a direct measure of the trap energy. We are planning to try this method soon, using a Nernst glower

and a set of III - V and II - VI semiconducting compounds as filters.

We now return to Figure 1 and consider the shapes of the trapping portion of the curves. The calculation by Wertheim[2] considers a single trap having zero cross-section for carriers of one sign and a temperature-independent constant for the others, in conjunction with a single recombination center. Where increases with decreasing temperature, a semilog plot should give a straight line whose slope is either the trap energy or the difference in energy between the trap and the recombination level, depending on the temperature dependence of the recombination center. The non-agreement of the curves in Figure 1 with this prediction could be due to more than one trap, temperature-dependent cross-sections, interaction of several recombination levels with one trap, or a combination of these factors. The $652^{o}K$ curve indeed suggests that more than one recombination level exists, but the change in slope of the $480^{o}K$ and $601^{o}K$ curves at 1000/T - 8.5 suggests the presence of more than one trap (in rough analogy with Figure 2). We must emphasize, however, that the decays were quite exponential at all temperatures, in contrast with Baicker's results on silicon. More will be said about this later. With regard to the $400^{o}K$ curve, the deviation from non-linearity is greater at high temperatures, which would be consistent with a cross-section varying as some negative power of T. The problem is obviously complex enough that none of these possibilities can be ruled out at this time.

We plan to measure τ vs. injection level at several temperatures, which can be used to check the variation of the cross-sections with temperature.[9]

In view of the above factors, it is difficult to distinguish between the traps which anneal strongly between 400°K and 480°K and those which come in at 480°K - 600°K. In the range $6 < \frac{1000}{T} < 8$ it appears that the latter may be somewhat deeper but we must be aware of the pitfalls suggested by Figure 2 in assigning real meaning to the slopes over a limited temperature range. In general, the shapes are the same up to the 400°K anneal, which suggests either that one trap predominates or that if there are several, they anneal at the same rate up to 400°K. The former possibility is considered more likely.

Summarizing briefly, the annealing can be considered in several phases. Up to 390°K, about 0.5% of the trapping behavior anneals, with no apparent change in process. At the same time, roughly 60% of the radiation-induced recombination behavior is removed, but it is not known whether this is a true annealing or merely due to the minimum in $\ln \tau$ vs. 1/T moving to higher temperature as the traps go out. In the range 400°K to 480°K, both effects are reduced by $\sim$ 15%, with some change observed in the shapes of the trapping behavior. From 480°K to 600°K, the trapping behavior <u>increases</u> to within 0.5% of what it was immediately after irradiation, accompanied by an 18% recovery in recombination behavior. A possible mechanism for this has been given. Finally, at 652°K, the sample is essentially back to its pre-irradiation

condition. (Recall that it has now been removed from the cryostat and etched six times.) We plan to study this material further with the improved equipment now at our disposal.

In another experiment, two more samples from the same ingot were irradiated at 300°K, one with 3×10^{12} e/cm^2 at 55 Mev, the other with 2×10^{13} e/cm^2 at 10 Mev. Oscillograms were taken at 85°K and plotted in the manner given by Baicker[4] to determine the trap energy and density. This is shown in Figure 4. First, we note that for the two room-temperature samples there is some fast initial recombination observed at 85°K, whereas in the low-temperature-irradiated sample the decay was exponential. Second, if this data is analyzed in terms of Figure 1 of Reference 4, the trap energy is $0.14 \pm .01$ ev from a band edge and the introduction rate is a factor of 10 larger for the high-energy run, namely 1.5 cm^{-1} as opposed to 0.16 cm^{-1} at 10 Mev. Quantitative results cannot be obtained for the low-temperature-irradiated sample since its lifetime is completely unresolvable. A slope of ~ 0.14 ev is not inconsistent with the low-temperature portion of Figure 1, and also this sample should have about 10^2 more traps than the high-energy room temperature irradiated one which explains why the lifetime is completely swamped by the trapping effects. We conclude that these traps, which anneal below 400°K, are associated with a complex defect produced in greater number by higher energy electrons.

We have alluded to several experiments we plan for the near future. In addition, we plan to simultaneously irradiate a

bridge sample and a lifetime sample cut from the same portion of an ingot in an attempt to correlate annealing of conductivity, mobility, trapping and recombination. It was felt that measuring lifetime on a bridge sample would lead to excessive difficulty masking the electrodes from the 150 KVP X-rays.

References

[1]J. A. Hornbeck and J. R. Haynes, Phys. Rev. 97, 311 (1955).

[2]G. K. Wertheim, Phys. Rev. 109, 1086 (1958).

[3]Progress Reports covering periods 15 September 1963 to 15 March 1964 and 15 March 1964 to 15 September 1964 for NASA Grant NsG-290.

[4]J. A. Baicker, Phys. Rev. 129, 1174 (1963).

[5]O. L. Curtis, Jr., and J. H. Crawford, Jr., Phys. Rev. 124, 1731 (1961).

[6]W. Shockley and W. T. Read, Phys. Rev. 87, 835 (1952).

[7]O. L. Curtis, Jr., and J. H. Crawford, Jr., Phys. Rev. 126, 1342 (1962).

[8]G. D. Watkins and J. W. Corbett (private communication).

[9]J. S. Blakemore, Semiconductor Statistics, Pergamon Press, New York (1962), p. 269.

III. Infrared Properties of 60 Mev Electron-Irradiated Silicon

J. F. Becker

In previous progress reports we presented results on the effects of $\sim$40 Mev electrons on the infrared properties of floating zone (low oxygen concentration $\lesssim 10^{16}$ cm^{-3}) and pulled (high oxygen concentration $\gtrsim 10^{17}$ cm^{-3}) silicon. In an attempt to study the problem further and to investigate the possible energy dependence of the radiation-induced defect infrared bands, we recently completed a series of detailed annealing experiments on 60 Mev electron-irradiated silicon. (Sample temperature during irradiation was $\lesssim 300^{\circ}$K.)

Experimental Results:

The characteristics of the silicon samples studied together with the incident electron energy, resistivity values before and after irradiation, total integrated fluxes and sample thicknesses, are given in Table I. In all annealing results to be presented the sample was kept at temperature for twenty minutes, and the area under the radiation-induced absorption peak was taken to be a measure of the relative defect concentration.

Figure 5 shows the isochronal annealing results on the 1.8 μ defect absorption band for one floating zone and two pulled (oxygen containing) silicon samples. The relative defect concentration is plotted as a function of the annealing temperature in $^{\circ}$C. The three samples shown in Figure 5 also exhibit bands at 3.46 and 3.62 μ when the sample is cooled to 80°K. However,

the 3.46 and 3.62 μ bands are not seen when monochromatic light is used, indicating that we are observing different states of ionization of the defect responsible for the 1.8, and the 3.46, 3.62 μ bands. In each case the 3.46 and 3.62 μ bands anneal out at the same temperatures as the 1.8 μ band. The isochronal annealing results for the 3.46 and 3.62 μ bands is shown in Figure 6. The defects responsible for the 1.8 μ band are always found to be produced more efficiently in oxygen-containing than in floating zone silicon.

The longest wave length defect absorption bands observed in silicon were in the 9 - 12 μ region. These very sharp bands at 11.6 μ and 12 μ were observed only in oxygen-containing silicon. Typical isochronal annealing results for pulled silicon are shown in Figure 7 where the relative defect concentration (area under absorption peak) vs. annealing temperature is displayed. The results given in Figure 7 are for a pulled (oxygen-containing) n-type silicon phosphorous doped sample (#2.1); similar results (see Figure 8) were observed for the pulled p-type silicon boron-doped sample (#1.1 - converted to n-type by the irradiation) described in Table I. From the results given in Figure 7, it can be seen that as the 11.6 and 12 μ bands approach complete annealing two other bands at 9.07 and 11.2 μ appear, approach maximum intensity at $\sim$450^{o}C, and finally disappear completely at 580 and 530^{o}C respectively.

Discussion of Results and Conclusions:

Fan and Ramdas[1] have observed the 1.8 μ band in oxygen-containing silicon irradiated by low energy electrons $E \lesssim 4.5$ Mev, 9.6 Mev deuterons, and reactor neutrons. However, in later work Fan and Ramdas[4] reported that the 1.8 μ band was not produced in floating zone silicon irradiated with 4.5 Mev electrons. As shown in Figure 5, the defect responsible for the 1.8 μ band absorption is produced in 60 Mev electron irradiation irrespective of the oxygen concentration. The only difference we have observed in 40 - 60 Mev electron irradiation of floating zone and pulled silicon is that the 1.8 μ band is produced more efficiently in the latter. Fan and Ramdas[4] argue that oxygen assists in the formation of the defect responsible for the absorption at 1.8 μ and that the defect center of the 1.8 μ band consists of a complex aggregate of simple defects formed more efficiently when many displacements are produced close to each other (say by 9.6 Mev deuterons, reactor neutrons, and 40 - 60 Mev electrons). The point is that the defect formation is assisted by the presence of oxygen atoms. The exact role of the oxygen is unknown.

The 1.8 μ band was shown by Fan and Ramdas[1] to be dependent upon the position of the Fermi level and is caused by one type of defect in different states of ionization. Moreover, both the 1.8 μ and the 3.46 and 3.62 μ bands are associated with energy levels at about E_c - 0.21 ev. The fact that we observe the 1.8 and the 3.46 and 3.62 μ bands annealing out together strongly suggests they are associated with the same defect. From their

results, Fan and Ramdas[1] deduced that the 1.8 μ absorption is not seen if the 0.21 level is occupied by electrons and had not determined whether the 1.8 μ band is observed with a Fermi level close to the valence band. Recently we have examined this point experimentally and have found evidence for the 1.8 μ band in irradiated (50 Mev electrons) silicon that was still p-type after irradiation (see Section V of this report).

If one compares the annealing of the 864 cm^{-1} (Si-A center) radiation-induced oxygen vibrational band in Figures 7 and 8 to the annealing of the 1.8 μ band (Figure 5) for samples #2.1 and #1.1, there is a strong suggestion that as the 1.8 μ band anneals at 250 - 300°C, the Si-A center concentration (834 cm^{-1} band) increases slightly, implying that vacancies and/or oxygen atoms from the annealing 1.8 μ center are producing additional oxygen-vacancy complexes. We have observed this same effect in all annealing experiments performed on oxygen containing silicon, which tends to give additional credence to the conclusion that oxygen atoms may be involved in the defect aggregate giving the 1.8 μ absorption.

From a series of isothermal anneals at 140°C, 170°C and 200°C on the 1.8 μ band, Fan and Ramdas[1] concluded that the recovery was governed by a simple monomolecular process having an activation energy of 0.8 ev. This conclusion does not appear to agree with our results of Figure 5. In all of our annealing results on the 1.8 μ band there appear to be at least two distinct stages of annealing (see Figure 5, which is a typical example),

implying a more complex annealing behavior than found by Fan and Ramdas,[1] consistent with the conclusion that the defect responsible for the 1.8 μ band is a complex aggregate which one would not expect to follow a single activation energy monomolecular process.

The annealing behavior of the Si-A center at 834 cm^{-1} shown for typical oxygen-containing pulled crystals in Figures 7 and 8 is very similar to what has been observed by Corbett, Watkins, Chrenko and McDonald,[2] and by Corbett, Watkins and McDonald[6] who used 1.4 Mev electrons in their irradiation. Corbett et al.[2, 6] do not report evidence for the bands at 864 and 1103 cm^{-1}, whereas Ramdas and Fan[5] have observed the 864 cm^{-1} and 834 cm^{-1} band in neutron-irradiated silicon. We have found that the production of the 864 cm^{-1} band is flux dependent, reaching maximum intensity at $\sim 2 \times 10^{18}$ e/cm^2 (40 - 60 Mev), decreasing with further irradiation and finally disappearing after $\sim 6 \times 10^{18}$ e/cm^2. We conclude that the 834, 864, 894 and 1103 bands shown in Figures 7 and 8 are all defect vibrational bands associated with oxygen.

The growth of the 894 cm^{-1} band as the Si-A center (834 cm^{-1}) anneals out (see Figures 7 and 8) was first observed by Corbett et al.[3] and reported by them in more detail later[6] for 1.4 Mev electron-irradiated oxygen-containing silicon. In addition to the 894 cm^{-1} band Corbett et al[6] found three other new bands appearing in the range 887 - 1000 cm^{-1} after the A center anneals. We do not observe any evidence for growth of bands other than the 894 cm^{-1} and 1103 bands between 800 and 1103 cm^{-1} shown in

Figures 7 and 8. The appearance of satellite and growth bands between 800 and 1000 cm^{-1} has also been observed by Ramdas and Fan[5] in reactor neutron irradiated silicon containing dispersed oxygen. However, Ramdas and Fan[5] do not report any detailed annealing studies of the growth and satellite bands.

The Si-A center at 834 cm^{-1} was first shown by Watkins, Corbett and Walker[7] to be associated with the net acceptor level at E_c - 0.17 ev found from the electrical properties of irradiated oxygen-containing silicon. Saito, Hirata and Horiuchi[9] observed the 0.17 ev level from carrier concentration measurements in Co^{60} gamma (1.25 Mev) and 2 Mev electron irradiation of pulled silicon. Recent annealing experiments in our laboratory by Merrill on 1.4 Mev electron irradiation of pulled silicon have shown the same annealing behavior for the 0.17 ev level as given in Figures 7 and 8 for the A center at 834 cm^{-1}. In our laboratory, Cheng has also observed the 0.17 ev level in 45 Mev electron-irradiated pulled silicon from electrical properties.

Corbett et al.,[2] and Watkins et al.[8] have shown that the 834 cm^{-1} band (Si-A center) is an oxygen vibrational band due to an oxygen atom coupled to a vacancy and is the dominant defect in irradiated oxygen-containing silicon. Corbett et al.[6] have suggested a tentative model for the growth of the 894 cm^{-1} band as the Si-A center anneals. They proposed a model in which the oxygen-vacancy complex (comprising the Si-A center) "diffuses" through the lattice as a unit until another isolated interstitial oxygen atom becomes attached to the complex. Then the new defect

involves the association of two oxygen atoms and one vacancy and would give rise to one additional vibrational band. Upon further heating an additional oxygen is united to the O_2-vacancy pair, causing the emergence of other growth bands. Although speculative, the model appears to describe qualitatively the complex atom movements occuring during annealing. No model has been suggested to account for either the 864 cm^{-1} or 1103 cm^{-1} bands shown in Figures 7 and 8.

Table I

Sample Characteristics, Incident Electron Energy, Resistivity Values, Total Integrated Flux and Thickness of Samples Studied

Sample No.	Type and Impurity	Resistivity* Before Irradiation (ohm-cm)	Resistivity* After Irradiation (ohm-cm)	Crystal Growing Method	Incident Energy (Mev)	Total Integrated Flux e/cm^2	Thickness (mm)
1.1	p-type Si+ Boron	100 Ω-cm	2.9×10^5 Ω-cm	Pulled	60	2.5×10^{18}	6.33
2.1	n-type Si Phosphorous	100 Ω-cm	2.7×10^5 Ω-cm	Pulled	60	2.5×10^{18}	5.26
3.1	n-type Si Phosphorous	1.0 Ω-cm	6×10^4 Ω-cm	Floating zone	60	1.3×10^{18}	5.97

*Pre-irradiation value @ $300^{\circ}K$.

+n-type after irradiation (from Hall effect measurements).

References

[1] H. Y. Fan and A. K. Ramdas, Jour. Appl. Phys. 30, 1127 (1959).

[2] J. W. Corbett, G. D. Watkins, R. M. Chrenko, and R. S. McDonald, Phys. Rev. 121, 1015 (1961).

[3] G. D. Watkins, J. W. Corbett, and R. S. McDonald, Bull. Am. Phys. Soc. 5, 26 (1960).

[4] H. Y. Fan and A. K. Ramdas, Proc. of the Int'l Conf. on Semiconductor Physics, Prague (1960), p. 309.

[5] A. K. Ramdas and H. Y. Fan, Jour. Phys. Soc. Japan 18, Suppl. II, 33 (1963).

[6] J. W. Corbett, G. D. Watkins, and R. S. McDonald, Phys. Rev. 135, (5A) 1381 (1964).

[7] G. D. Watkins, J. W. Corbett, and R. M. Walker, Journ. Appl. Phys. 30, 1198 (1959).

[8] G. D. Watkins and J. W. Corbett, Phys. Rev. 121, 1001 (1961).

[9] H. Saito, M. Hirata, and T. Horiuchi, Jour. Phys. Soc. Japan 18, Suppl. II, 246 (1963). Earlier references to electrical properties of irradiated silicon are cited in this paper.

IV. 15 - 50 Mev Electron Irradiation of Germanium at 300°K*

A. Kalma

Room temperature electron irradiation of various germanium samples was carried out at both ≈15 Mev and ≈50 Mev. Temperature dependence of the resistivity and carrier concentration of each sample was measured at various times during the irradiation. A list of the samples and the irradiation history of each one is given in Table II. The numbering system used in this table is the same as that used in the figures for this section. A curve labeled n on a figure corresponds to a measurement made after the irradiation labeled n for the corresponding sample in the table.

On the n-type samples, there was no dopant effect and on the p-type samples, there was no energy effect, so only one set of figures of resistivity and carrier concentration vs. 1/T is included for each type. Figures 9 and 10 are for n-type Ge, first irradiated with Co^{60} photons and then with ≈50 Mev electrons. Figures 11 and 12 are for n-type Ge, first irradiated with Co^{60} photons and then with ≈15 Mev electrons. Figures 13 and 14 are for n-type Ge only irradiated with ≈15 Mev electrons. Figures 15 and 16 are for n-type Ge only irradiated with ≈ 50 Mev electrons. Figures 17 and 18 are for p-type Ge

---

*Preliminary results from these experiments were previously reported in the Progress Report covering the period from 15 March 1964 to 15 September 1964, "Radiation Damage to Semiconductors by High-Energy Electron and Proton Radiation", John C. Corelli. These experiments were conducted in cooperation with John W. Cleland of the Solid State Division of the Oak Ridge National Laboratory, Oak Ridge, Tennessee.

irradiated with $\approx$15 Mev electrons.

The annealing and then re-irradiation of the Co^{60} irradiated samples was to ascertain if there was any dopant effect in the results.

The energy difference on the n-type samples is obvious. As can be seen by comparing Figures 10 and 12, the higher energy electrons raise the hole concentration from the post Co^{60}-γ irradiation level considerably more than the lower energy electrons. The former also lowers the slope of the carrier concentration a great deal more than the latter. Further irradiation still increases the hole concentration for the 50 Mev sample and lowers it for the 15 Mev sample. This same trend can be observed after the annealing of the samples. After converting the samples to p-type, the 50 Mev electrons raise the hole concentration and the 15 Mev electrons lower it. The higher energy electron results are similar to neutron results suggesting that 50 Mev electrons produce disorder regions like neutrons do and these raise the hole concentrations and affect the apparent energy level of the defect. The 15 Mev electrons do not produce any amount of disordered regions, if they produce any. The same general conclusion can be drawn from the 30 Ω-cm samples. From Figure 14, it can be seen that 15 Mev electron irradiation converted the n-type sample to p-type and then raised the hole concentration slightly to a saturation point and further irradiation left it almost unchanged. Whereas, on Figure 16, a sample irradiated with 50 Mev electrons, the hole concentration on the p-type side

continues to rise with further irradiation. Again, there is the energy difference in the results where the effects of disordered regions can be seen on the higher energy sample and is much less on the lower energy sample.

The results on the originally p-type samples were the same regardless of energy. In Figure 18 it can be seen that electron irradiation raised the hole concentration slightly and then saturation was reached. The work on the n-type samples is considered to be complete. Further work on p-type germanium may be started later.

Table II

Doping, Resistivity and History of

Room Temperature Irradiated Germanium Samples

Sample	Type	No	Energy (Mev)	History Total Flux (e/cm^2)	
As6#1	Ge-N(As)-10Ω-cm	I	——	Unirradiated	(n-type)
		II	1.25	2×10^{18} (Co^{60} photons)	(p-type)*
		III	55	5×10^{14}	(p-type)
		IV	46	5.8×10^{15}	(p-type)
		V	Annealed for 20 hours at 450°C		(n-type)
		VI	50	5.7×10^{16}	(p-type)
As6#2	Ge-N(As)-10Ω-cm	I	——	Unirradiated	(n-type)
		II	15	4.3×10^{16}	(p-type)
Sb6#1	Ge-N(Sb)-10Ω-cm	I	——	Inirradiated	(n-type)
		II	1.25	2×10^{18} (Co^{60} photons)	(p-type)*
		III	15	8×10^{14}	(p-type)
		IV	17	3.3×10^{16}	(p-type)
		V	Annealed for 20 hours at 450°C		(n-type)
		VI	15	4.3×10^{16}	(p-type)
		VII	15	9.2×10^{16}	(p-type)
Sb6#2	Ge-N(Sb)-10Ω-cm	I	——	Unirradiated	(n-type)
		II	1.25	8×10^{16} (Co^{60} photons)	(p-type)*

*The Co^{60} photon irradiations were performed by John W. Cleland of the Solid State Division, Oak Ridge National Laboratory, Oak Ridge, Tennessee.

Sample	Type	No	Energy (Mev)	History Total Flux (e/cm^2)	
		III	45	5×10^{14}	(p-type)
		IV	46	5.3×10^{15}	(p-type)
		V	Annealed for 20 hours at 450°C		(n-type)
		VI	50	5.7×10^{16}	(p-type)
SM40#1	Ge-N(Sb)-30Ω-cm	I	——	Unirradiated	(n-type)
		II	45	5×10^{14}	(p-type)
		III	46	5.3×10^{15}	(p-type)
		IV	50	3.4×10^{16}	(p-type)
SM40#2	Ge-N(Sb)-30Ω-cm	I	——	Unirradiated	(n-type)
		II	15	8×10^{14}	(p-type)
		III	17	3.3×10^{16}	(p-type)
		IV	15	8.6×10^{16}	(p-type)
		V	15	13.5×10^{16}	(p-type)
SM40#4	Ge-N(Sb)-30Ω-cm	I	——	Unirradiated	(n-type)
		II	55	5×10^{14}	(p-type)
		III	46	5.8×10^{15}	(p-type)
		IV	50	3.5×10^{16}	(p-type)
NCP1#12	Ge-P-30Ω-cm	I	——	Unirradiated	(p-type)
		II	46	5.5×10^{15}	(p-type)
NCPL#13	Ge-P-30Ω-cm	I	——	Unirradiated	(p-type)
		II	17	1.9×10^{16}	(p-type)
		III	15	6.2×10^{16}	(p-type)

V. Infrared Studies with 45 Mev Electron-Irradiated Oriented Single Crystal Silicon

Li-Jen Cheng and John F. Becker

Four samples of 100Ω-cm P-doped silicon were irradiated with 45 Mev electrons (two with an integrated flux of 3×10^{18} e/cm^2, the others with 6.5×10^{18} e/cm^2) at room temperature. The electron beam was incident in the $\langle 100 \rangle$ direction for two of the samples, and the other two samples were irradiated with the beam incident along the $\langle 110 \rangle$ direction. The infrared absorption of the radiation-induced 1.8 μ band was measured with the infrared beam incident along the $\langle 100 \rangle$ and $\langle 110 \rangle$ directions at room temperature using an AgCl polarizer. No significant dichroic ratio was observed in these samples. An experiment to find re-orientation of the defects under stress at higher temperature is underway. From this experiment we expect to investigate the anisotropy properties of the defects responsible for this 1.8 μ absorption band.

In the room temperature irradiated pulled silicon samples (P-doped) three weak vibrational bands at 933 cm^{-1}, 937 cm^{-1} and 1022 cm^{-1}, in addition to the two vibrational bands at 834 cm^{-1} and 865 cm^{-1} reported previously, have been observed. We can conclude that all the centers causing these bands must be associated with oxygen atoms in the crystal, since none of these bands have been observed in irradiated floating zone silicon samples of similar resistivity and chemical impurity.

In Figure 19 the absorption coefficients of 834, 865

and 1022 cm^{-1} bands are plotted as a function of integrated electron flux.

The intensity of 834 cm^{-1} band (due to the Si-A center) monotonically increases with flux and also shows a tendency to reach a saturation value. This is not the case for 865 and 1022 cm^{-1} bands, which show that the absorption increases with flux initially, then appears to reach a maximum (at $\sim 2 \times 10^{18}$ e/cm^2), finally decreasing with increasing flux. This result suggests that the defects associated with these two bands may be formed by primary radiation defects and oxygen complexes, such as, a vacancy trapped by two or more oxygen atoms together, or, in the simplest case, the formation of an A center with one or more oxygen atoms nearby. Using this hypothesis, we may explain the decrease of the 865 cm^{-1} bands in such a way that the probability for the oxygen atoms nearby to form an A center with a vacancy becomes higher with increasing dose because of the exhaustion of the free interstitial oxygen atoms. If this suggested mechanism is operative, one would observe a decrease in the 865 cm^{-1} and 1022 cm^{-1} bands.

The intensity of the 933 cm^{-1} band was also observed to decrease with dose after an integrated flux of 2×10^{18} e/cm^2, but the 937 cm^{-1} band appears to increase slowly with dose up to 6.5×10^{18} e/cm^2; however, these two bands are very weak, making interpretation difficult.

In conclusion, one may say that the production of the various types of the centers corresponding to these bands depends on the condition of oxygen atoms in the crystal. This may explain in

part the reason that the number of radiation-induced oxygen-associated vibrational bands observed between 9 and 13 micron are different for various incident radiation particle and energy reported by others.[1, 2, 3, 4]

One sample of $\approx 0.01\Omega$-cm As-doped silicon (floating zone) irradiated at room temperature to a total integrated flux of 2×10^{18} e/cm^2 45 Mev electrons was measured with infrared absorption at liquid nitrogen temperature. In addition to 1.8 μ at 3.3 μ defect bands previously reported, there are several bands observed in the range from 4 μ to 8 μ (see Figure 20). The absorption change from 1600 to 2500 cm^{-1} probably corresponds to the broad 5.5 μ band observed by H. Y. Fan and A. K. Ramdas, J. Appl. Phys. 30, 1127 (1959). However some fine structure was observed in the present work. A new band at 1207 cm^{-1} (8 μ) was observed in this As-doped sample, which disappears when a germanium filter is placed in the infrared beam in front of the sample. The band reappears when the sample is illuminated with a flash light. The centers associated with these bands must be associated with impurity atoms (As) since none of these bands has been observed in the samples of higher resistivity (0.1Ω-cm and higher). None of these bands has been observed at room temperature so the absorptions would be caused by electronic excitation.

For more information about the impurity effect on irradiation-induced infrared absorption bands in Si, further experiments are

needed and will be started in the next six month period.

One sample of floating zone silicon (B-doped) irradiated to a total integrated flux of 6.5×10^{18} e/cm^2 with 45 Mev electrons at 310°K was studied. The sample was still p-type after irradiation and exhibited both the 1.8 μ and the 3.9 μ bands when the infrared spectra were measured at 300°K and at 80°K. These bands have been reported by Fan and Ramdas in reactor neutron-irradiated p-type samples of low resistivity. Further annealing experiments are planned for these samples in the next six month period.

References

[1] J. W. Corbett, G. D. Watkins, R. M. Chrenko, and R. S. McDonald, Phys. Rev. 121, 1015 (1961).

[2] H. Y. Fan and A. K. Ramdas, Proc. of the Int'l Conf. on Semiconductor Physics, Prague (1960), p. 309.

[3] J. C. Corelli, G. C. Oehler, J. F. Becker, and K. J. Eisentraut, to be published in J. Appl. Phys (May 1965).

[4] See Section III of this report, "Infrared Properties of 60 Mev Electron-Irradiated Silicon" by J. F. Becker.

VI. Recovery of Carrier Concentration and Conductivity from 80°K to 360°K in n-type Silicon after 45 Mev Electron Irradiation

Li-Jen Cheng, O. H. Merrill, and A. Kalma

The results given in this section are an extension of previous studies to higher purity silicon. One sample of 100Ω-cm arsenic-doped pulled silicon was irradiated at 80°K with 44 Mev electrons to a total integrated flux of 2.7×10^{13} e/cm^2. An isochronal annealing experiment was carried out between 80°K to 360°K using temperature pulses of 10 minute duration similar to the experiments described in a previous progress report covering the period 15 March 1964 to 15 September 1964.

The gross features of the recovery behavior of the damage are found to be similar to that which we have observed in lower resistivity (lower purity) silicon doped with phosphorous. The fraction of damage remaining in carrier concentration after successive anneals plotted as a function of annealing temperature is given in Figure 21.

In order to investigate the properties of the radiation-induced defects in n-type Si in more detail, two silicon samples, one 16Ω-cm P-doped floating zone crystal and the other an 11Ω-cm P-doped pulled crystal, were irradiated at 15°K in our liquid helium cryostat to a total integrated flux of about $\sim 3 \times 10^{14}$ e/cm^2. (Due to technical difficulty in beam alignment, this flux measurement is quoted with a $\pm$ 30% accuracy.) Since the resistivities of these samples are too high and their variations due to temperature are too large at $\approx$15°K, we could not perform the measurements

accurately enough, and the damage produced by irradiation was measured only after the samples had been warmed up to the liquid nitrogen temperature. An isochronal annealing experiment was carried out between 80°K and 360°K using successive temperature pulses of 10 min. duration. The damages produced were 47% in carrier concentration, n, 65% in conductivity, σ for the floating zone sample and 67% in n, 69% in σ for the pulled crystal sample. The fraction of damage remaining in carrier concentration of the two samples is plotted as a function of the successive annealing temperature and is shown in Figure 22. The measurements are made at a reference temperature of 80°K after each anneal. The floating zone sample did not show any clear annealing stage as was obtained in the samples cut from same ingot and irradiated at 80°K, but it only exhibited a rather broad anneal from 80°K to 300°K. The recovery curve of the reciprocal Hall mobility $\frac{1}{\mu}$ of the sample shows no definite structure as that of the sample irradiated at 80°K (see Figure 23). The total percentage of carrier recovery up to 350°K in the sample irradiated at 15°K was about 38%.

The recovery of the pulled crystal sample appeared to be in three stages as shown in the samples irradiated at 80°K (Figure 22), but there was only a small reverse annealing observed at about 240°K, and the amount annealed out between 260°K and and 350°K also became smaller.

By comparison of the data from 15°K and 80°K irradiations, we may conclude that formation of defects induced by 45 Mev electron at 15°K are not the same as those induced at 80°K.

In these experiments we have observed that there is some temperature dependence of formation of certain irradiation-induced defects. For example, the defects causing 240°K reverse annealing and 290°K annealing in the pulled crystal are not primary defects produced by irradiation but are defects formed by combinations of oxygen atoms and the primary irradiation-induced defects (probably vacancies). Since, in the formation of those defects, there must be some irradiation-induced defect able to migrate at the irradiation temperature in order to meet the oxygen atom, this should cause the temperature-dependence of the formation. It was suggested for low-energy electron irradiation by Wertheim (Wertheim, G. K., Phys. Rev. 115, 568 /T959/) and Mackay and Klontz (Mackay, J. W., Klontz, E. E., J. Appl. Phys. 30, 1269 /T959/) that the increase in efficiency of the production of defects with increasing temperature could be explained by assuming that the primary displacement event results in a metastable configuration of a vacance-interstitial pair. This metastable pair may then be thermally excited over a recombination barrier to annihilate the pair or over a liberation barrier to form stable defects. This concept regarding thermal barriers may be applied to high-energy electron irradiation in order to explain the temperature dependence of formation of certain irradiation-induced defects.

The experimental results suggest strongly that some primary radiation-induced defects are not stable below liquid nitrogen temperature. From spin resononance work (G. D. Watkins, Jour.

Phys. Soc. Japan 18, Suppl. II, 22 [1963]; G. D. Watkins, J. W. Corbett, and R. M. Walker, J. Appl. Phys. 30, 1198 [1959], and G. D. Watkins' paper given at the Paris, France, Radiation Damage Symposium [July 1964]), it is well known that the vacancy in n-type silicon becomes mobile at about 60°K. Since the annealing temperature of the A center is about 340°C, it is possible that the defects which correspond to the annealing stage at 290°K are formed by oxygen atoms and some primary irradiation-induced defects, besides vacancies, which are mobile below 80°K. The possibility that the 290°K annealing stage is related to the oxygen-enhanced annealing, such as the annealing of the divacancy in Si (G. D. Watkins, to be published in Phys. Rev.) and the 1.8 u radiation-induced infrared band (J. C. Corelli, G. Oehler, J. F. Becker, and K. J. Eisentraut, to be published in J. Appl. Phys. [May 1965]) is ruled out, since there is no corresponding annealing stage in the floating zone sample. There are two possible explanations for the reverse annealing at about 240°K. One is that a dissociation of some complex defects produced favorably at 80°K irradiation occurred around that temperature, its fragments individually forming stable defects with some imperfections (probably oxygen atoms) existing in the pulled crystal only, which are able to trap carriers at liquid nitrogen temperature. The dissociating defects might exist in the floating zone crystal, but there are not enough oxygen atoms to form the stable defects to trap carriers, such as the A center. The other possible explanation may be as follows: This behavior

may occur in the case of annealing of donors whose levels lie in the forbidden band close to bottom of the conduction band. These centers are then almost completely ionized in samples at the temperature of liquid nitrogen and their annealing reduces the free-electron density. The annealing stage from 90°K to 220°K in the pulled crystal is not significantly different in 15°K and 80°K irradiations. In general, there are three annealing stages between 80°K to 350°K for n-type silicon irradiated by 45 Mev electrons at 80°K and 15°K. The percentages of recovery in carrier concentration in these three stages for various samples are summarized in Table III.

Table III

The percentages of carrier concentration recovery in the annealing stages from 80°K to 350°K for pulled crystal of n-type Si (1, 10 and 100Ω-cm).

Samples		% of Recovery			
		80°K to 220°K	220°K - 265°K	265°K to 350°K	Total up to 350°K
Si-N-1		31%	-6%	25%	50%
Si-N-10	80°K irradiated	33%	-4%	24%	53%
Si-N-100		22%	-4%	33%	51%
Si-N-10	15°K irradiated	37%	1%	14%	50%

From the above data, one may notice that there would be an

annealing stage which starts to appear at about an annealing temperature of 350°K. This may be due to the annealing stage of the E center (phosphorous-vacancy complex). After annealing up to about 360°K one of the predominant defects in pulled crystals remaining is the oxygen-vacancy complex (A center) which has an energy level about 0.17 ev below the conduction band (see Figure 24 of this report and Figure 33 of our previous progress report), for which the Kitovskii method was used to compute the value of the energy level (Kitovskii, Mashovets, and Ryvkin, Soviet Physics - Solid State 4, 2088 [T964]). From the temperature dependence curves of Figure 24, one may also infer that there might be some other defects annealed out around 290°K with an energy level, very roughly estimated to be at about 0.1 ev below the conduction band. The production rates of the defects with 0.17 ev energy level in various resistivity n-type silicon pulled crystals produced by 45 Mev electron irradiation at 80°K are roughly the same about $0.25 cm^{-1}$, but the production is about two times lower for 15°K irradiated 10Ω-cm silicon sample.

Wertheim and Buchanan (J. Appl. Phys. 30, 1232 [T959]) reported an anneal of mobility at 120°K in 1 Mev electron-irradiated P-doped silicon (floating zone crystal) with a flux of 6.0×10^{14} e/cm^2. Due to the low defect production rate in 1 Mev electron irradiation of silicon, their data can be used to compare to our sample irradiated with 6.4×10^{13} e/cm^2 even though this sample had more damage than that of Wertheim and

Buchanan. However, there was an annealing stage at about 125°K, during which 5% of the damage recovered in carrier concentration, but about 20% in $\frac{1}{\mu}$. This agrees qualitatively with Wertheim's data. Watkins found in his spin resonance work that the concentrations of the A center and of the E center increase in the temperature range from 200°K to 300°K (see previous page for references), and some unidentified spectra disappeared between 100°K to 200°K (private communication) in his low-energy electron-irradiated silicon. Unfortunately, there is no detailed work being reported on the annealing properties of low energy electron or gamma ray-irradiated Si from 80°K to room temperature. Therefore, it is impossible to make a comparison between the annealing behaviors of low energy and high energy electron-irradiated n-type silicon in order to ascertain which annealing stages are due to some characteristic defects caused by high energy electron irradiation only. This kind of work has been done on germanium. The reader is referred to:

1. Our previous Progress Report.
2. E. G. Wikner, Phys. Rev. 138A, 294 (1965).

In general, the percentage of damage annealed out for 45 Mev electron-irradiated n-type silicon is larger in $\frac{1}{\mu}$ than in n (see Table IV), which may suggest a possibility that most of the complex defects formed by high energy electron irradiation only are annealed out in the temperature below 350°K.

Table IV

Samples	% of Recovery	
	n	$1/\mu$
1Ω-cm Pulled	50%	55%
F. Z.	30%	55%
10Ω-cm Pulled	53%	70%
F. Z.	30%	72%
10Ω-cm Pulled	50%	85%

In Table IV, we note that the samples with higher resistivities had more recovery in $\frac{1}{\mu}$, which is another evidence supporting the imperfection dependence of annealing behavior of n-type Si in the temperature range from $80^{o}K$ to $350^{o}K$, which was mentioned in our previous report.

VII. Initial Studies of Defects Induced in 45 Mev Electron-Irradiated Silicon Using Photoconductivity as the Probe

Li-Jen Cheng

In this section we report on some preliminary results on measurements of photoconductivity spectra in n-type Si irradiated with 45 Mev electrons at room temperature ($296^{o}K$).

The samples were placed in a liquid nitrogen cryostat fitted with a NaCl window which could transmit infrared light. A modified Perkim-Elmer Model 12C infrared spectrometer was used as a source of monochromatic infrared light. In order to suppress parasitic scattered light, an Si filter was placed in the beam of light incident on the sample. The light intensities were measured by an infrared-detecting thermocouple, which is an integral part of the Model 12C infrared spectrometer.

The samples had dimensions of about 0.1 x 0.1 x 0.5 $in.^3$ and were cut from 100Ω-cm floating zone silicon doped with arsenic and phosphorous.

In Figure 25, the photoresponse (photo current/intensity of light) of each of the samples is plotted as a function of wave length. There were some essential differences found between the samples doped with P and As which are evident in the results shown in Figure 25. Both samples were irradiated with the same total integrated flux of 6×10^{14} e/cm^2. The photoconductive currents were measured using a Kethley electrometer, due to the high resistances of the samples at $80^{o}K$ after irradiation. There were two defect energy levels found in each sample. For

the sample doped with phosphorous the photon energies causing the defect photoconductivity are located at about E_c-0.4 ev and E_c-0.6 ev. However, the actual values of the threshold of defect photoconductivity were found to be very difficult to pinpoint from our recent data. The defects associated with an energy of 0.4 ev may be the phosphorous-vacancy complex (E center), found by spin-resonance and electrical property measurements since no such levels are observed in the arsenic-doped samples. There were also two steps in the photoconductivity spectra found in the irradiated samples doped with As (see Figure 25), which correspond to the threshold photon energies, at E_c-0.55 ev and tentatively at E_c-0.75 ev.

Measurement of the kinetics in photoconductivity of the irradiated samples has been started. The effects of infrared quenching and charge transfer were observed in 100Ω-cm P-doped floating zone silicon irradiated with 45 Mev electrons. A systematic investigation of infrared quenching and charge transfer phenomena is underway in order to find the actural cause for these effects.

A low-noise, high input impedance amplifier capable of measuring a signal of 10^{-8} volt at a 13 cycle/sec frequency is under construction in an attempt to improve the sensitivity of our measurement. We have also concluded that a double pass single beam infrared monochromator is needed to improve our energy resolution.

Figure Captions

Fig. 1 Carrier lifetime τ vs. $1000/T(^{o}K)$ for an 8.5 ohm-cm antimony-doped germanium sample irradiated at $86^{o}K$ by 50 Mev electrons. The temperature dependence of τ is shown before irradiation and after various anneals at the indicated temperatures.

Fig. 2 Calculated carrier lifetime, τ , vs. $1000/T(^{o}K)$ for an n-type germanium sample containing 10^{14} electrons/cm^3 using Shockley-Read[6] analysis applied to two independent recombination levels.

Fig. 3 Isochronal annealing of traps and recombination centers of 50 Mev electron-irradiated 8.5 ohm-cm antimony-doped germanium. (See Text for discussion and explanation of symbols.)

Fig. 4 Photo-induced excess carrier concentration plotted vs. decay time for two 8.5 ohm-cm antimony-doped germanium samples irradiated at $300^{o}K$ by 10 and 55 Mev electrons.

Fig. 5 Isochronal annealing of the 1.8 μ band for two pulled silicon samples (sample #1.1 and #2.1) and one floating zone silicon sample (#3.1). Fraction of damage remaining is plotted vs. annealing temperature. All measurements were made at $296^{o}K$. (See Table I for further details of samples.)

Fig. 6 Isochronal annealing of the 3.6 and 3.4 μ bands for two pulled silicon samples (#1.1 and #2.1) and one floating zone silicon sample (#3.1). All measurements made at $80^{o}K$. (See Table I for further details of samples.)

Fig. 7 Isochronal annealing of radiation-induced oxygen-defect lattice vibrational bands vs. annealing temperature for a pulled n-type silicon sample (#2.1). In addition to the

anneal of the 834 cm^{-1} (12 u) and 864 cm^{-1} (11.6 u), the growth and decay of two other bands at 894 cm^{-1} (11.2 u) and 1103 cm^{-1} (9.07 u) is also included. All measurements were made with sample at 80°K. (See Table I for sample details.)

Fig. 8 Isochronal annealing of radiation-induced oxygen-defect lattice vibrational bands vs. annealing temperature for a pulled p-type (before irradiation) silicon sample #11. All measurements were made with sample at 80°K. (See Table I for sample details.)

Fig. 9 Carrier concentration vs. 1000/T for Ge(As) 10Ω-cm n-type irradiated with 50 Mev electrons at 320°K.

Fig. 10 Resistivity vs. 1000/T for Ge(As) 10Ω-cm n-type irradiated with 50 Mev electrons at 320°K.

Fig. 11 Carrier concentration vs. 1000/T for Ge(Sb) 10Ω-cm n-type irradiated with 15 Mev electrons at 320°K.

Fig. 12 Resistivity vs. 1000/T for Ge(Sb) 10Ω-cm n-type irradiated with 15 Mev electrons at 320°K.

Fig. 13 Carrier concentration vs. 1000/T for Ge(Sb) 10Ω-cm n-type irradiated with 15 Mev electrons at 320°K.

Fig. 14 Resistivity vs. 1000/T for Ge(Sb) 10Ω-cm n-type irradiated with 15 Mev electrons at 320°K.

Fig. 15 Carrier concentration vs. 1000/T for Ge(Sb) 10Ω-cm n-type irradiated with 50 Mev electrons at 320°K.

Fig. 16 Resistivity vs. 1000/T for Ge(Sb) 10Ω-cm n-type irradiated with 50 Mev electrons at 320°K.

Fig. 17 Carrier concentration vs. 1000/T for Ge 30Ω-cm p-type irradiated with 15 Mev electrons at 320°K.

Fig. 18 Resistivity vs. 1000/T for Ge 30Ω-cm p-type irradiated with 15 Mev electrons at 320°K.

Fig. 19 Flux dependence of absorption coefficients of several radiation-induced oxygen vibrational bands in pulled silicon irradiated with ~ 45 Mev electrons.

Fig. 20 Infrared spectra from 1600 to 2500 cm^{-1} of 45 Mev electron-irradiated silicon of initial 0.01 Ω-cm resistivity.

Fig. 21 Fraction of damage remaining in carrier concentration $\frac{\Delta n}{\Delta n_i}$ vs. annealing temperature (10 minute isochronal anneals) after 44 Mev electron irradiation at 80°K of 100 Ω-cm arsenic-doped pulled silicon. Total integrated flux = 2.7×10^{13} e/cm^2.

Fig. 22 Fraction of damage remaining in carrier concentration $\frac{\Delta n}{\Delta n_i}$ vs. annealing temperature (10 minute isochronal anneals) after 45 Mev electron irradiation at ~ 15°K of 11 Ω-cm phosphorous-doped pulled and floating zone silicon. Total integrated flux ~ 3×10^{14} e/cm^2.

Fig. 23 Fraction of damage remaining in reciprocal Hall mobility $f(1/\mu)$ vs. annealing temperature (10 minute anneals) after 45 Mev electron irradiation at ~ 15°K and at 80°K of 10 Ω-cm (P-doped) floating zone silicon.

Fig. 24 Temperature dependence of carrier concentration after successive 10 minute anneals at the temperatures indicated for 100 Ω-cm arsenic-doped pulled silicon irradiated at 80°K with 44 Mev electrons.

Fig. 25 Photoconductivity spectrum measured at 80°K (DC photocurrent per unit light intensity vs. wavelength)

for two 100 Ω-cm As-doped and one 100 Ω-cm P-doped floating zone silicon samples irradiated at 320°K with 48 Mev electrons. (The total integrated flux received by each sample is shown in the Figure.)

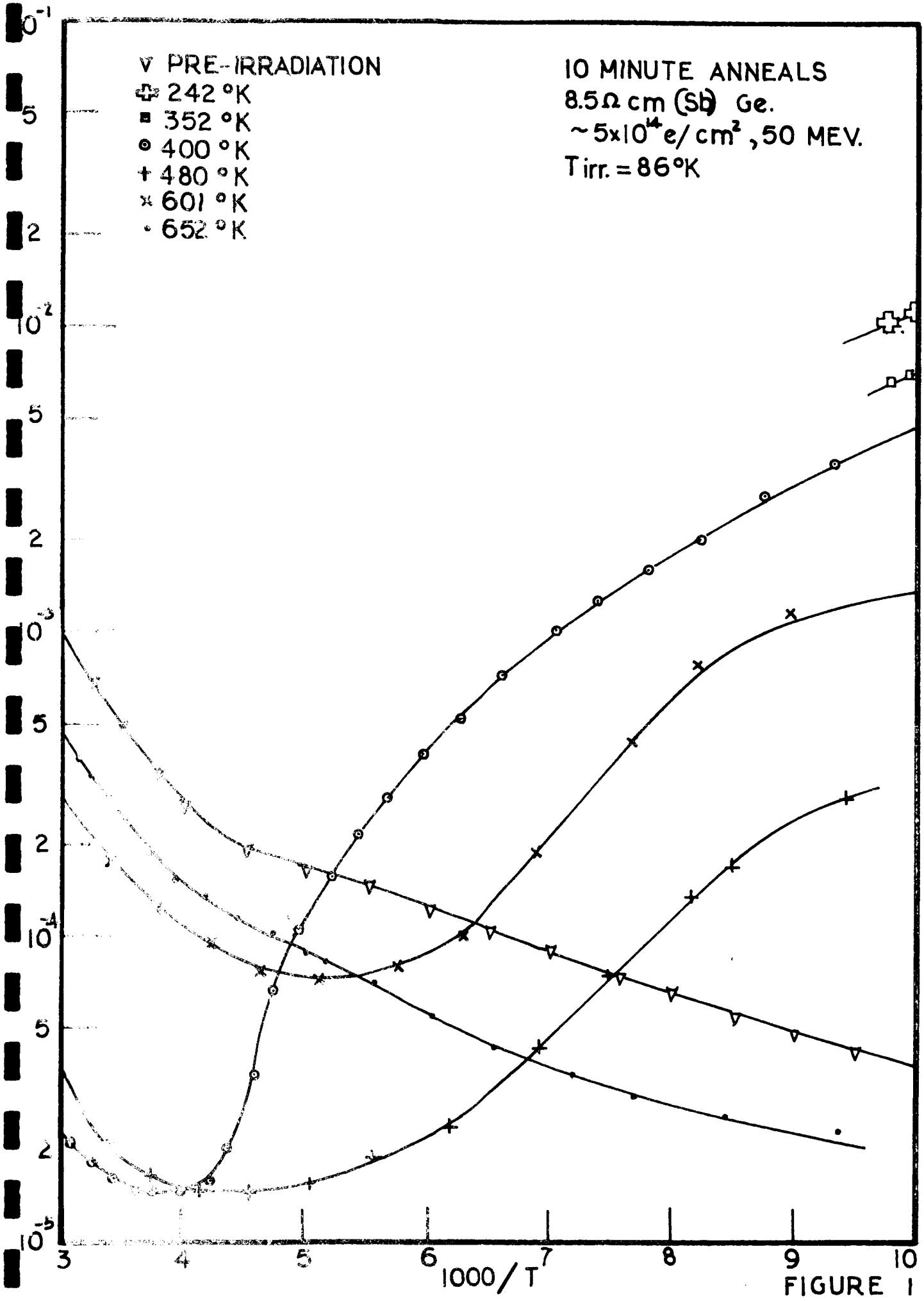
▽ PRE-IRRADIATION
242 °K
352 °K
400 °K
480 °K
601 °K
652 °K
10 MINUTE ANNEALS
8.5Ω cm (Sb) Ge.
~5x10^14 e/cm², 50 MEV.
T irr. = 86°K
10^-1
5
2
10^-2
5
2
10^-3
5
2
10^-4
5
2
10^-5
3
4
5
6
7
8
9
10
1000/T

FIGURE 1

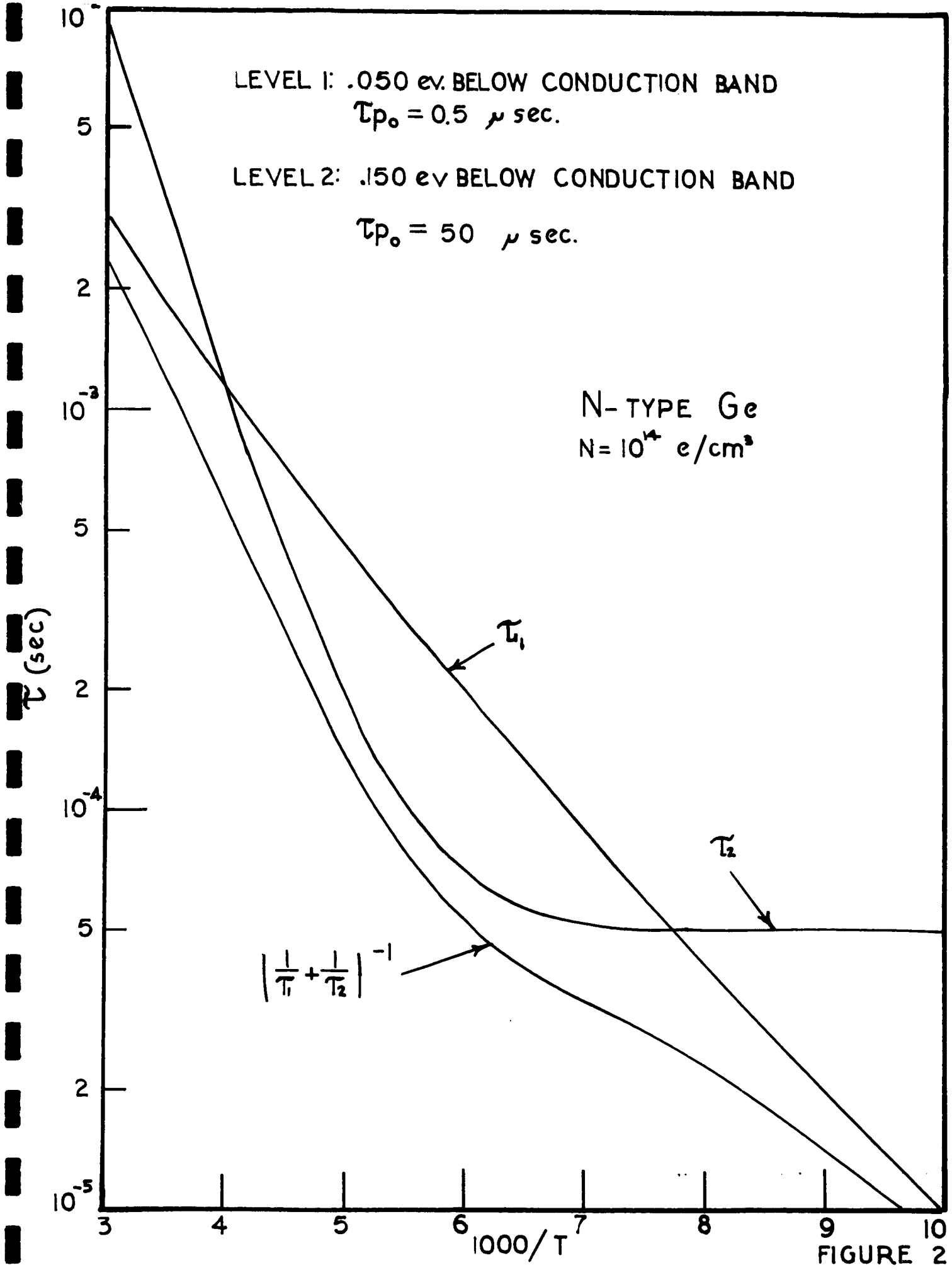
LEVEL 1: .050 ev. BELOW CONDUCTION BAND
$\tau p_o = 0.5$ μ sec.
LEVEL 2: .150 ev BELOW CONDUCTION BAND
$\tau p_o = 50$ μ sec.
N-TYPE Ge
N = 10^{14} e/cm³
τ_1
τ_2
$\left|\frac{1}{\tau_1}+\frac{1}{\tau_2}\right|^{-1}$
τ (sec)
10^{-}
5
2
10^{-3}
5
2
10^{-4}
5
2
10^{-5}
3
4
5
6
7
8
9
10
1000/T

FIGURE 2

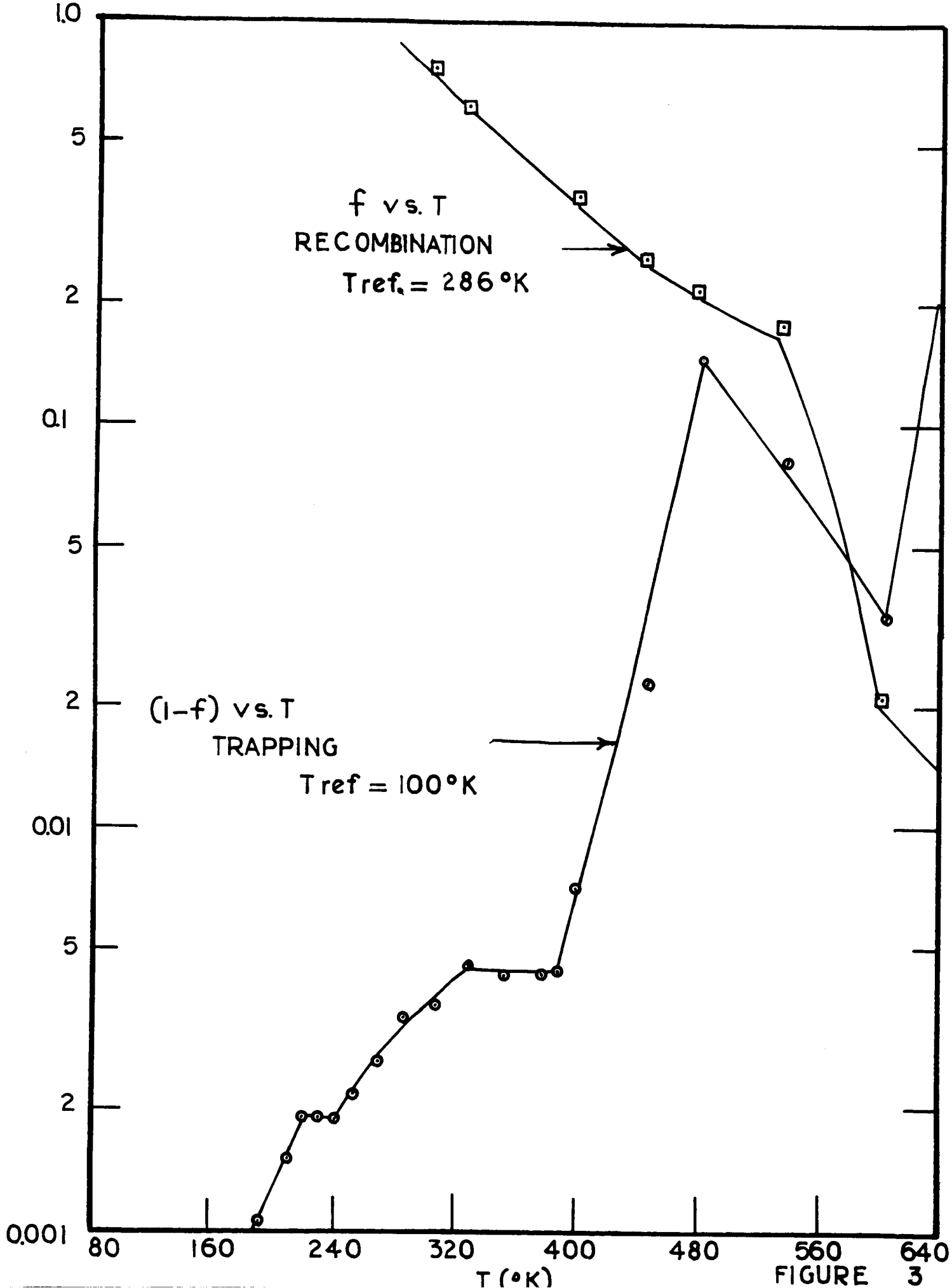
1.0
5
2
0.1
5
2
0.01
5
2
0.001
f vs. T
RECOMBINATION
Tref. = 286 °K
(1-f) vs. T
TRAPPING
Tref = 100 °K
80
160
240
320
400
480
560
640
T (°K)

FIGURE 3

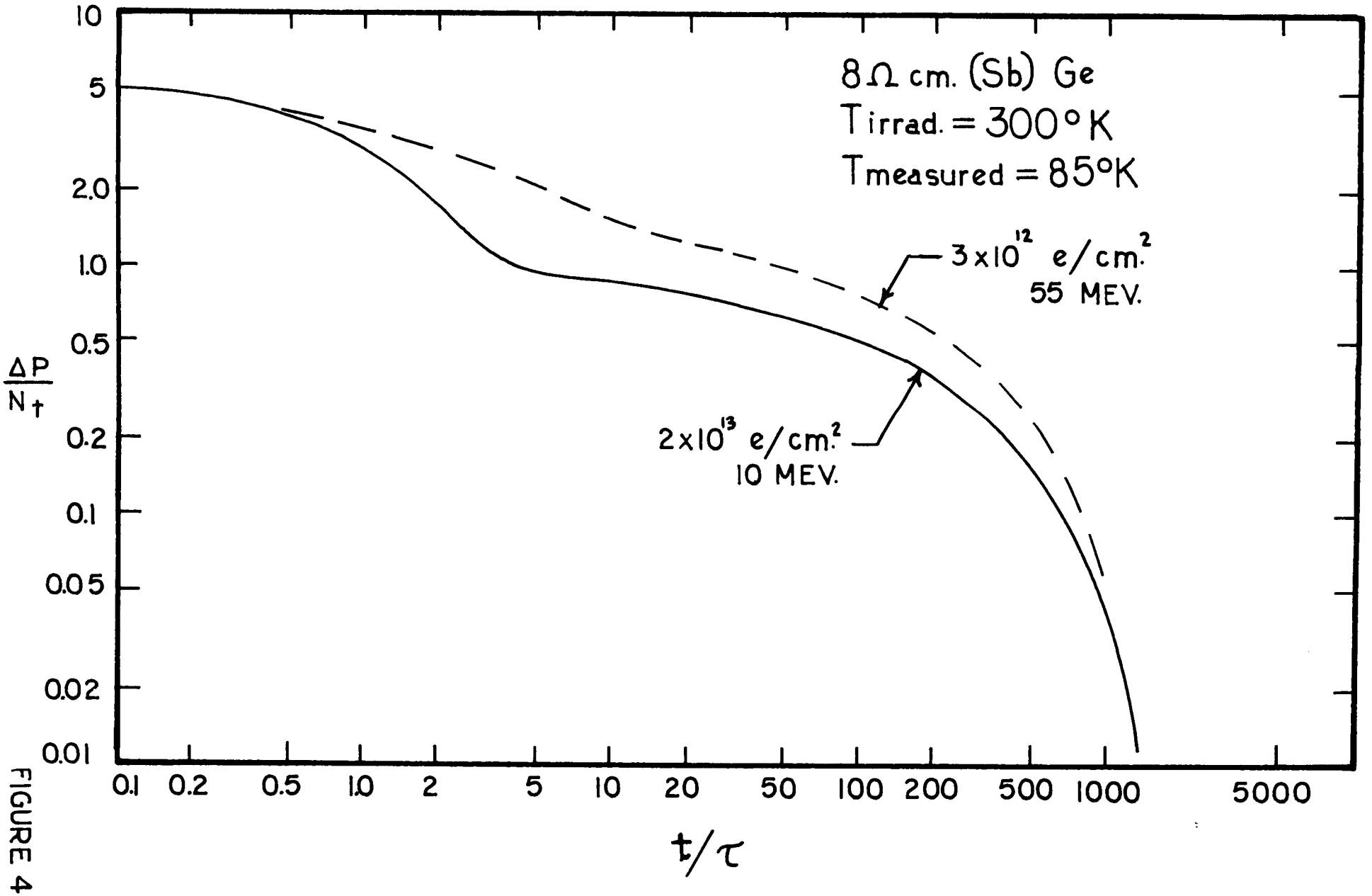
8 Ω cm. (Sb) Ge
T irrad. = 300° K
T measured = 85° K
3 x 10^12 e/cm.^2
55 MEV.
2 x 10^13 e/cm.^2
10 MEV.
ΔP / N t
t/τ
10
5
2.0
1.0
0.5
0.2
0.1
0.05
0.02
0.01
0.1
0.2
0.5
1.0
2
5
10
20
50
100
200
500
1000
5000

FIGURE 4

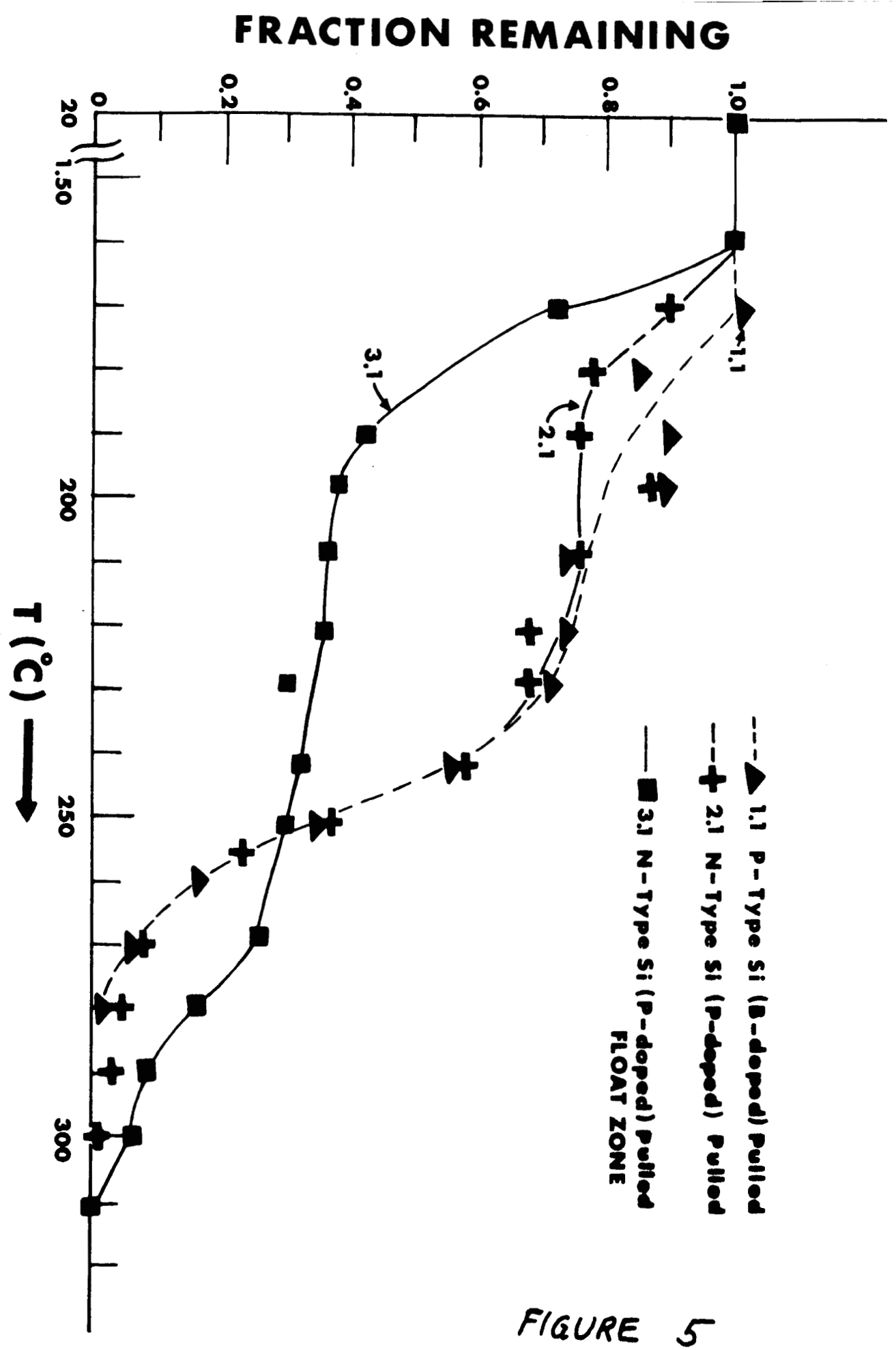
FRACTION REMAINING
0
0.2
0.4
0.6
0.8
1.0
20
1.50
200
250
300
T (°C)
1.1
2.1
3.1
1.1 P-Type Si (B-doped) Pulled
2.1 N-Type Si (P-doped) Pulled
3.1 N-Type Si (P-doped) Pulled FLOAT ZONE

FIGURE 5

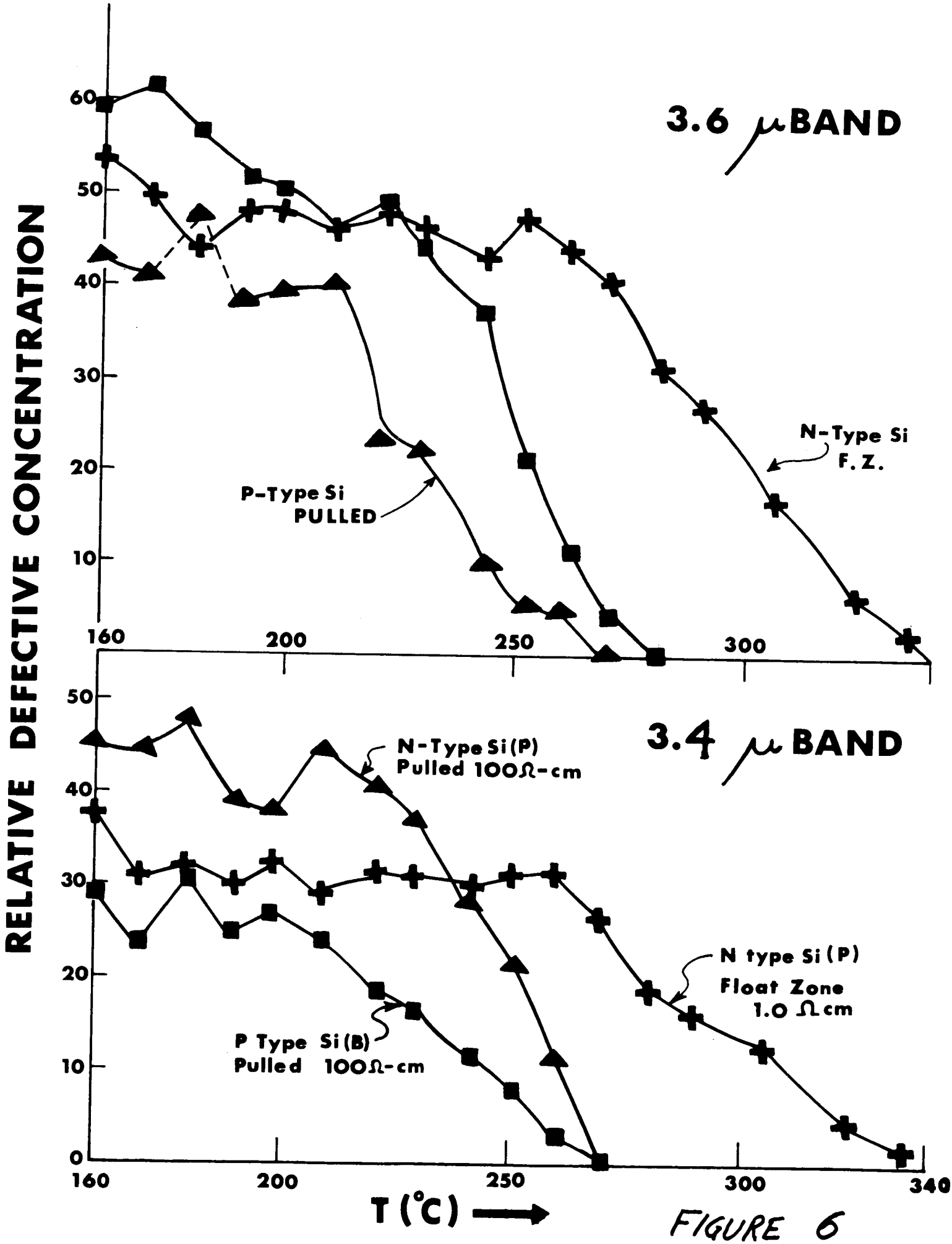
3.6 μBAND
RELATIVE DEFECTIVE CONCENTRATION
60
50
40
30
20
10
160
200
250
300
N-Type Si
F. Z.
P-Type Si
PULLED
3.4 μ BAND
50
40
30
20
10
0
N-Type Si(P)
Pulled 100Ω-cm
N type Si (P)
Float Zone
1.0 Ω cm
P Type Si(B)
Pulled 100Ω-cm
160
200
250
300
340
T (°C)

FIGURE 6

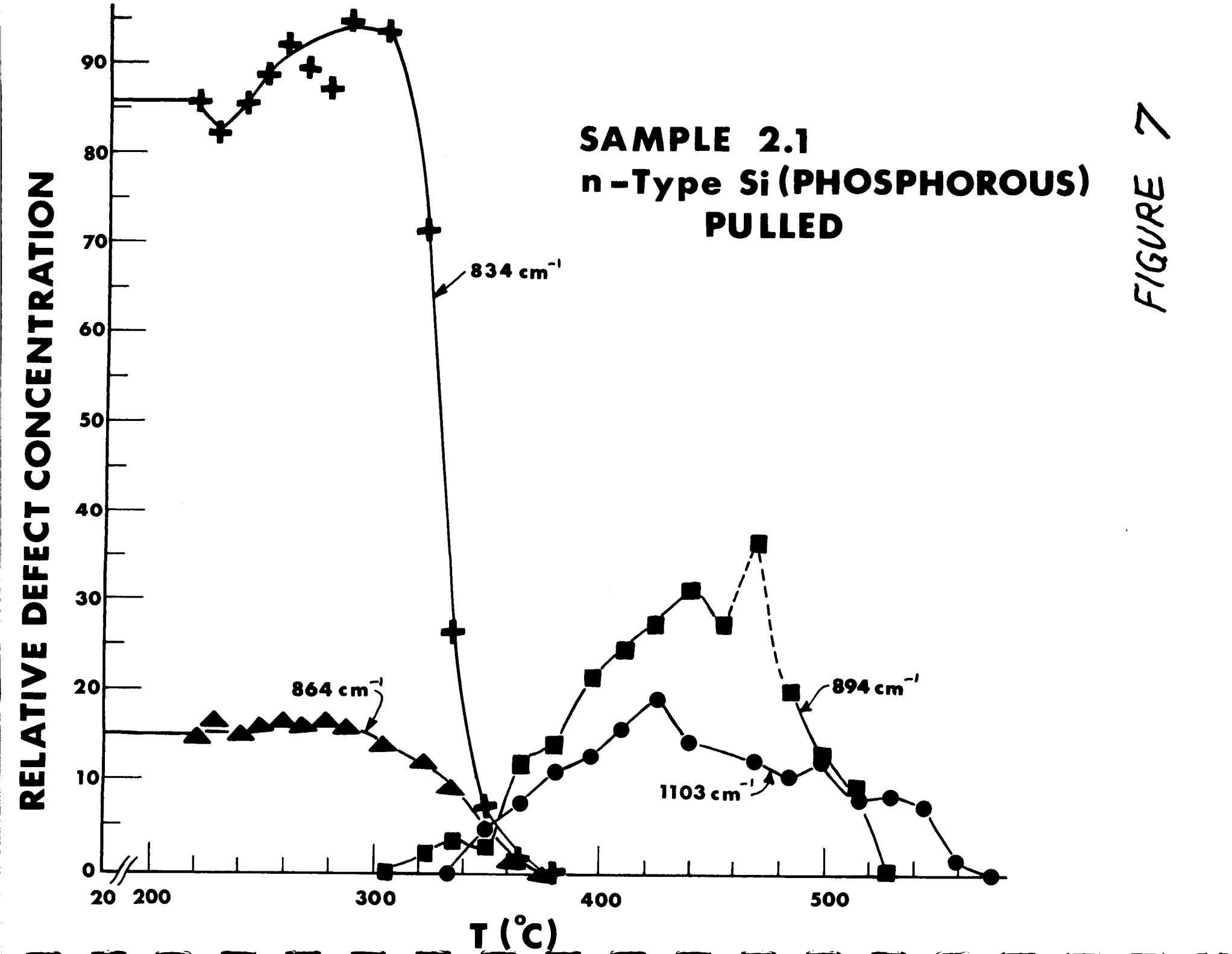
SAMPLE 2.1
n-Type Si (PHOSPHOROUS)
PULLED
RELATIVE DEFECT CONCENTRATION
T (°C)
834 cm⁻¹
864 cm⁻¹
894 cm⁻¹
1103 cm⁻¹
0
10
20
30
40
50
60
70
80
90
20
200
300
400
500

FIGURE 7

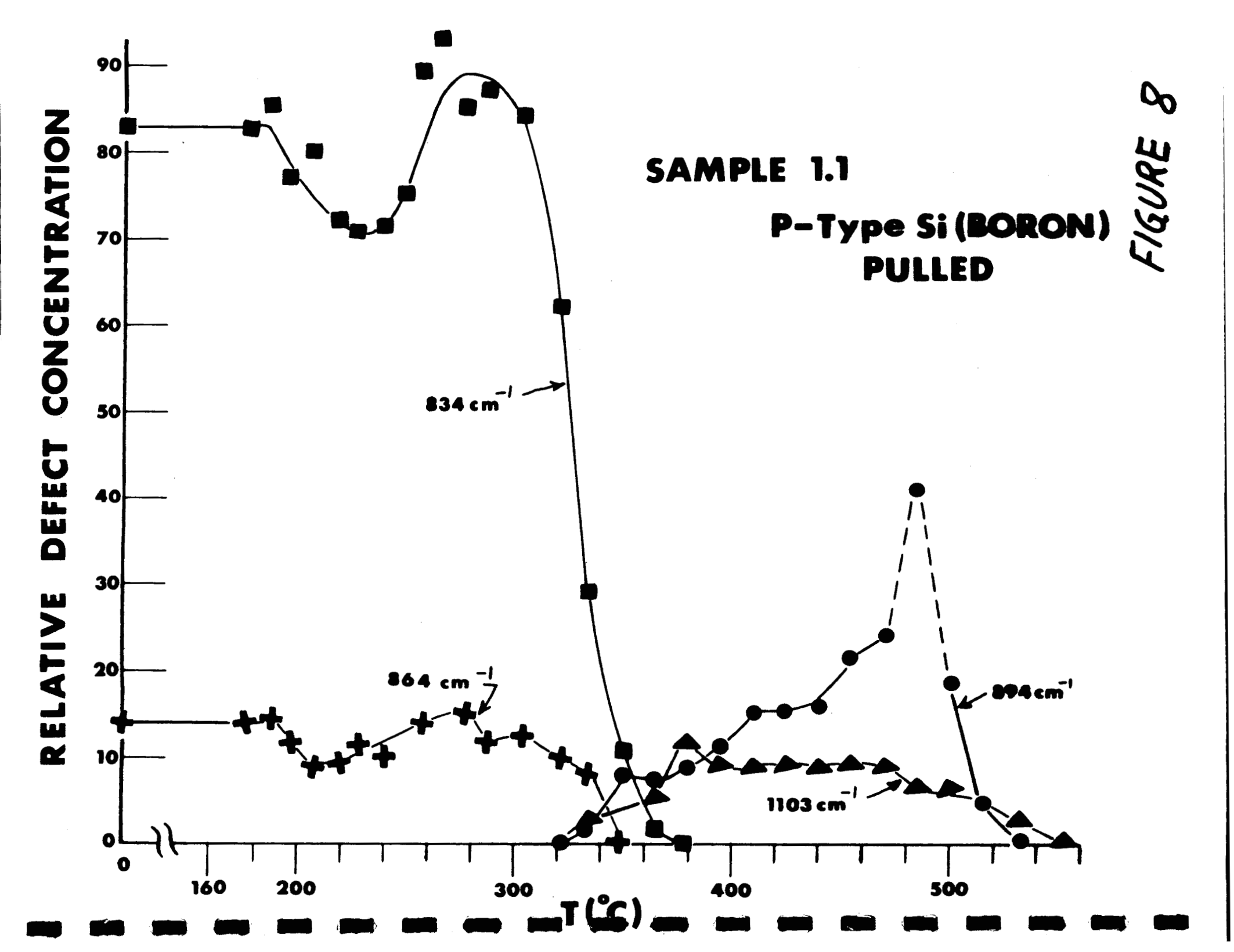
SAMPLE 1.1
P-Type Si (BORON)
PULLED
FIGURE 8
RELATIVE DEFECT CONCENTRATION
90
80
70
60
50
40
30
20
10
0
0
160
200
300
400
500
T (°C)
834 cm⁻¹
864 cm⁻¹
894 cm⁻¹
1103 cm⁻¹

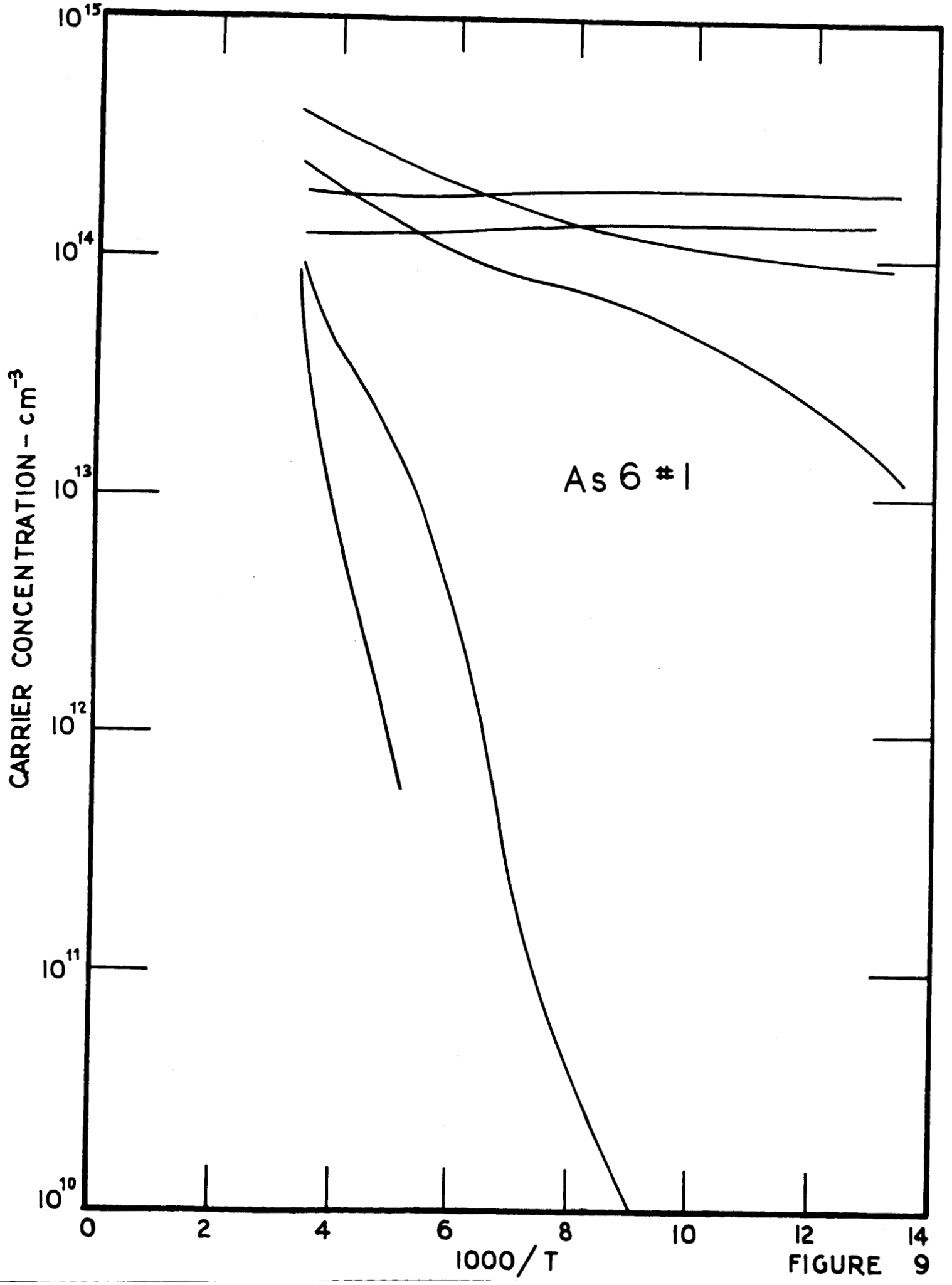
10^{15}
10^{14}
10^{13}
10^{12}
10^{11}
10^{10}
CARRIER CONCENTRATION - cm^{-3}
As 6 #1
0
2
4
6
8
10
12
14
1000/T

FIGURE 9

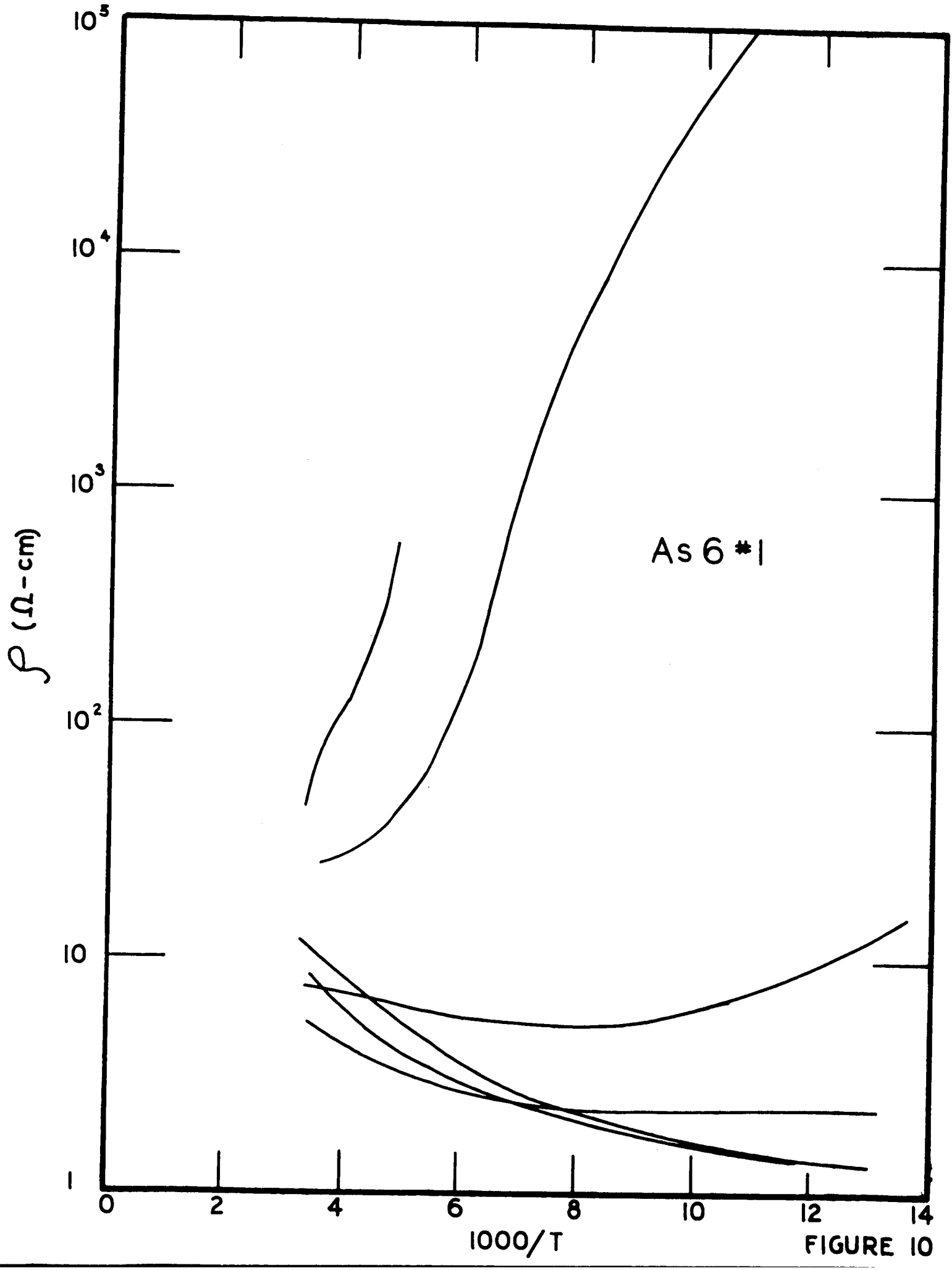

FIGURE 10

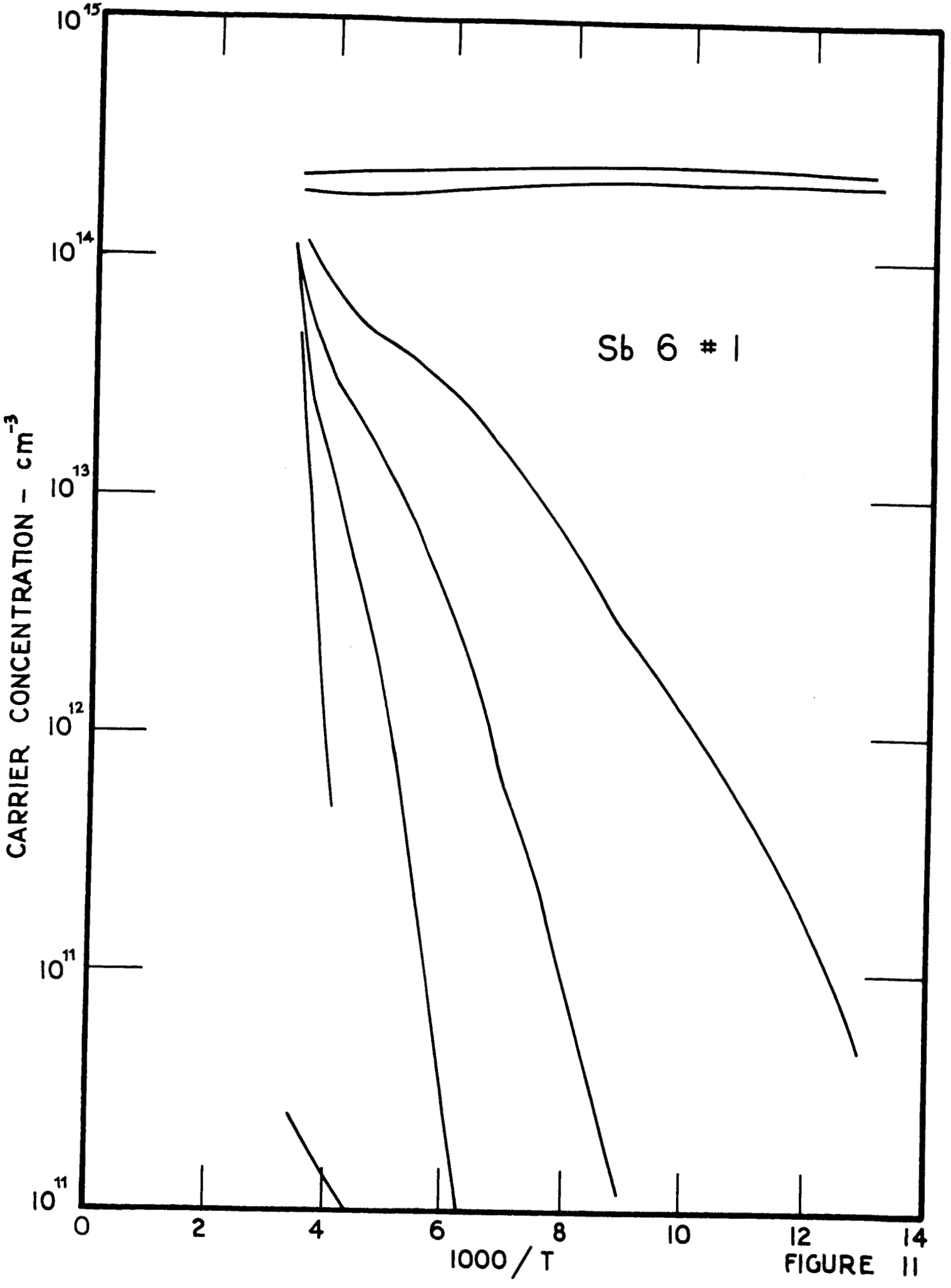
Sb 6 # 1
CARRIER CONCENTRATION - cm^{-3}
10^{15}
10^{14}
10^{13}
10^{12}
10^{11}
10^{11}
0
2
4
6
8
10
12
14
1000 / T

FIGURE 11

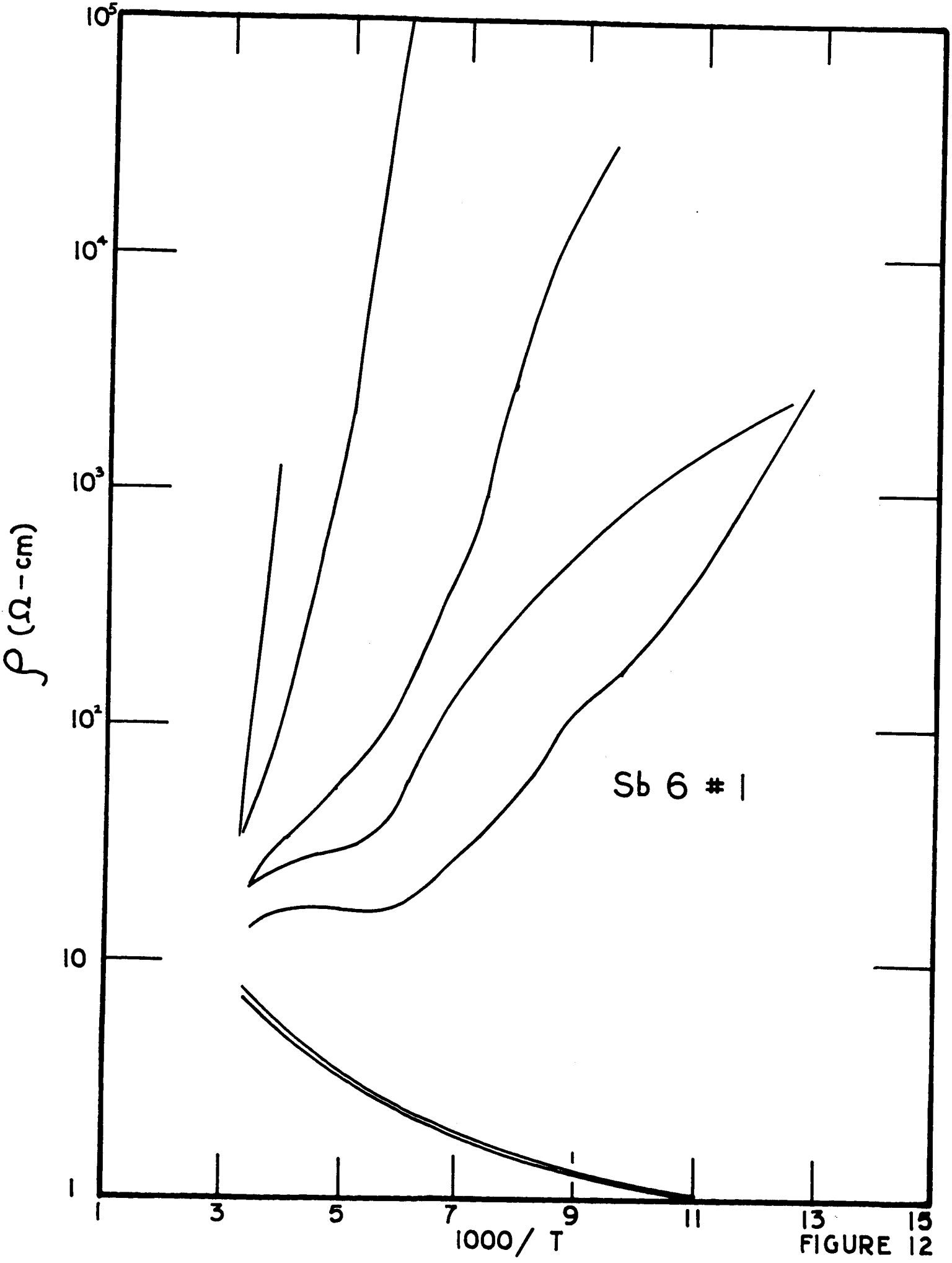

FIGURE 12

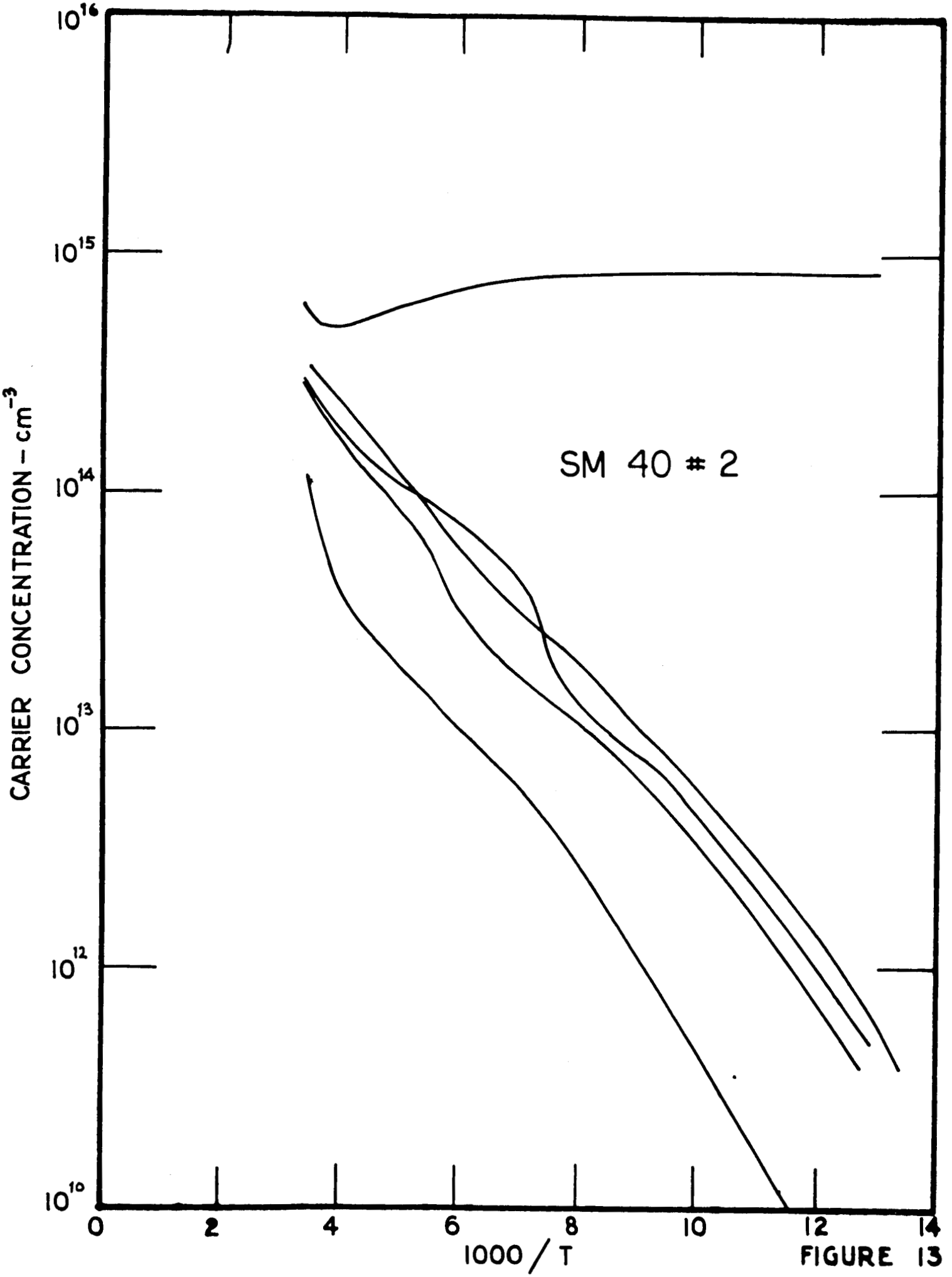
10^{16}
10^{15}
10^{14}
10^{13}
10^{12}
10^{10}
CARRIER CONCENTRATION - cm^{-3}
SM 40 # 2
0
2
4
6
8
10
12
14
1000 / T

FIGURE 13

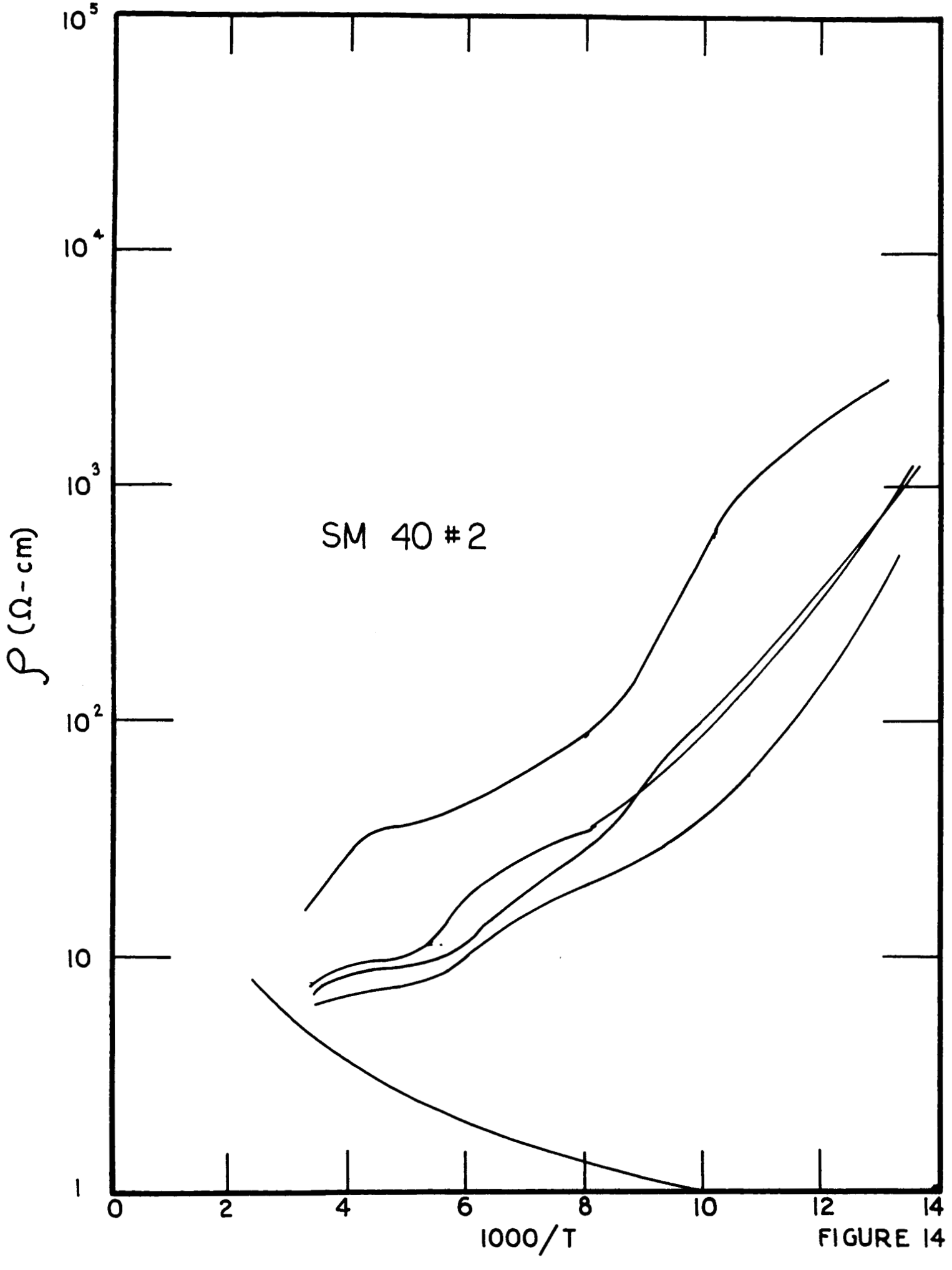

FIGURE 14

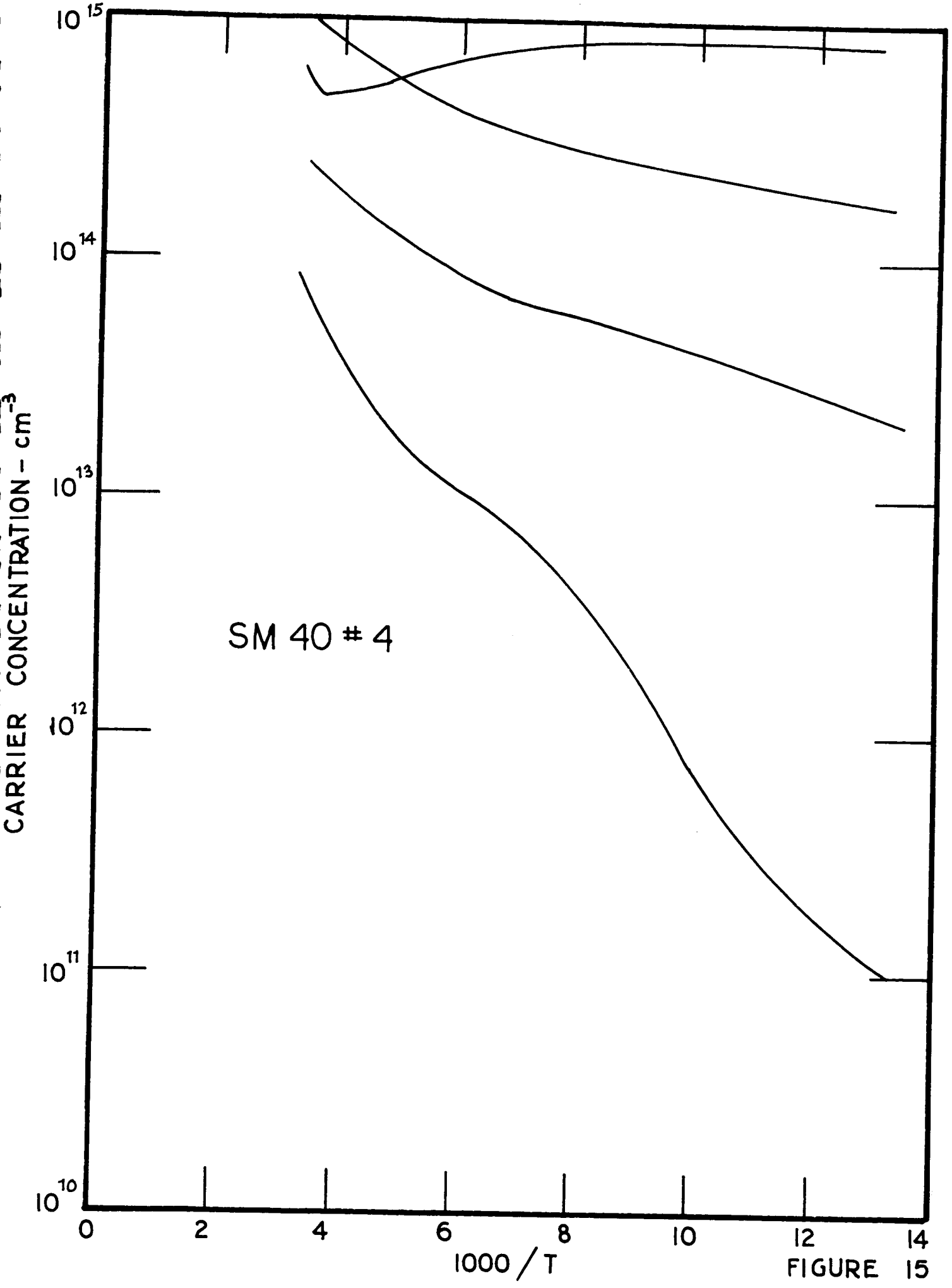
10^{15}
10^{14}
10^{13}
10^{12}
10^{11}
10^{10}
CARRIER CONCENTRATION - cm^{-3}
SM 40 # 4
0
2
4
6
8
10
12
14
1000 / T

FIGURE 15

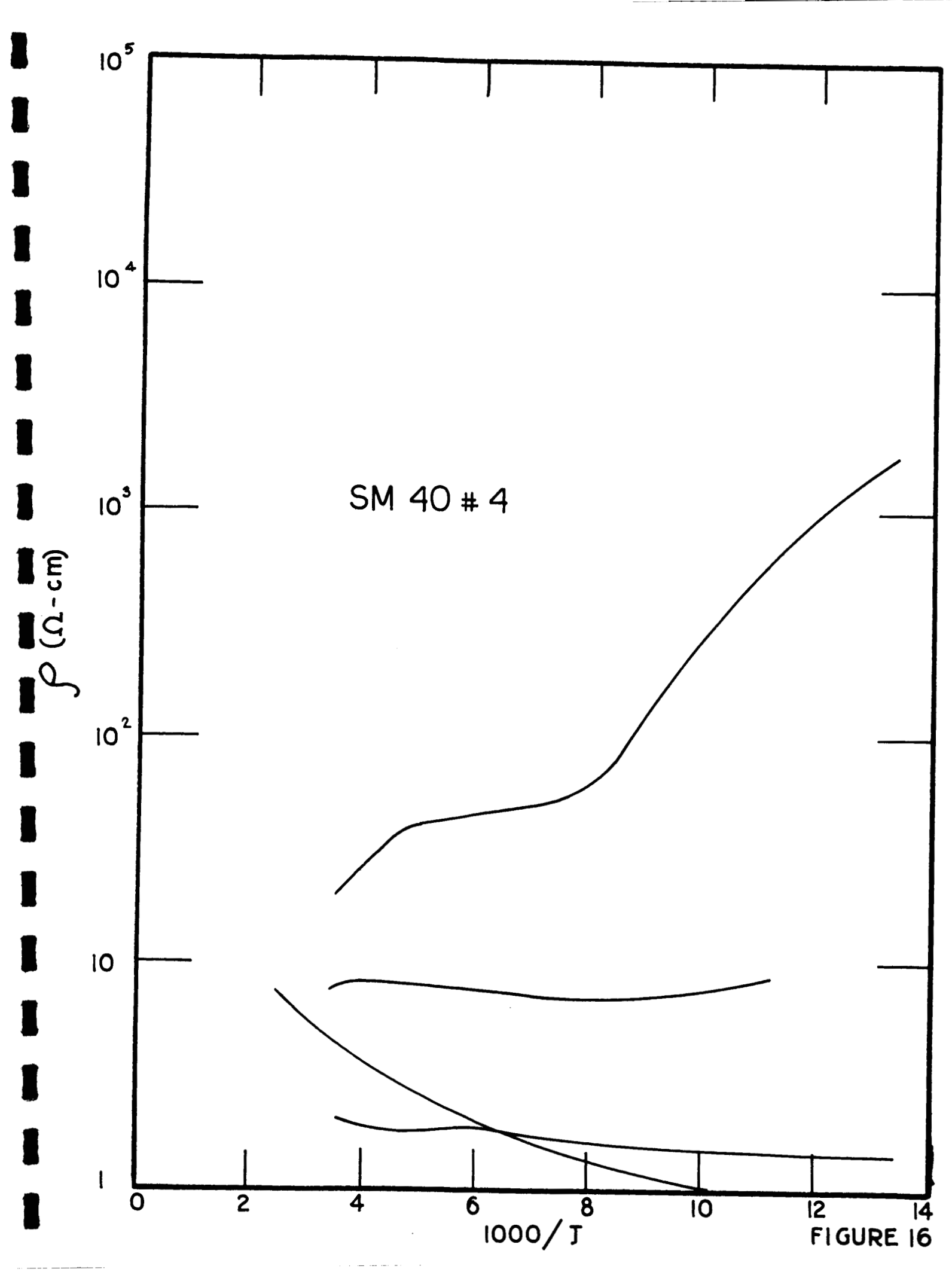

FIGURE 16

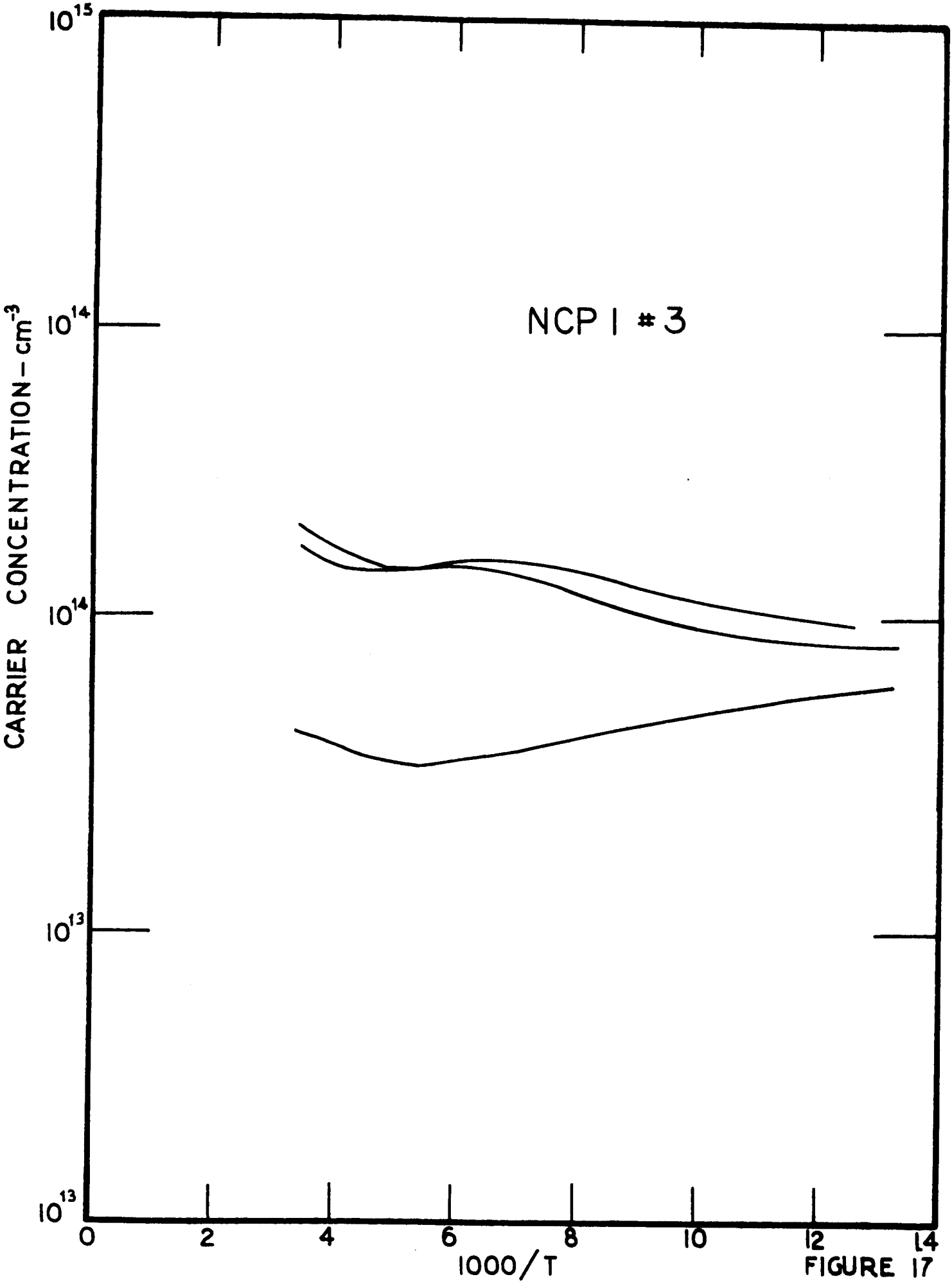
NCP I #3
CARRIER CONCENTRATION - cm⁻³
10¹⁵
10¹⁴
10¹⁴
10¹³
10¹³
0
2
4
6
8
10
12
14
1000/T

FIGURE 17

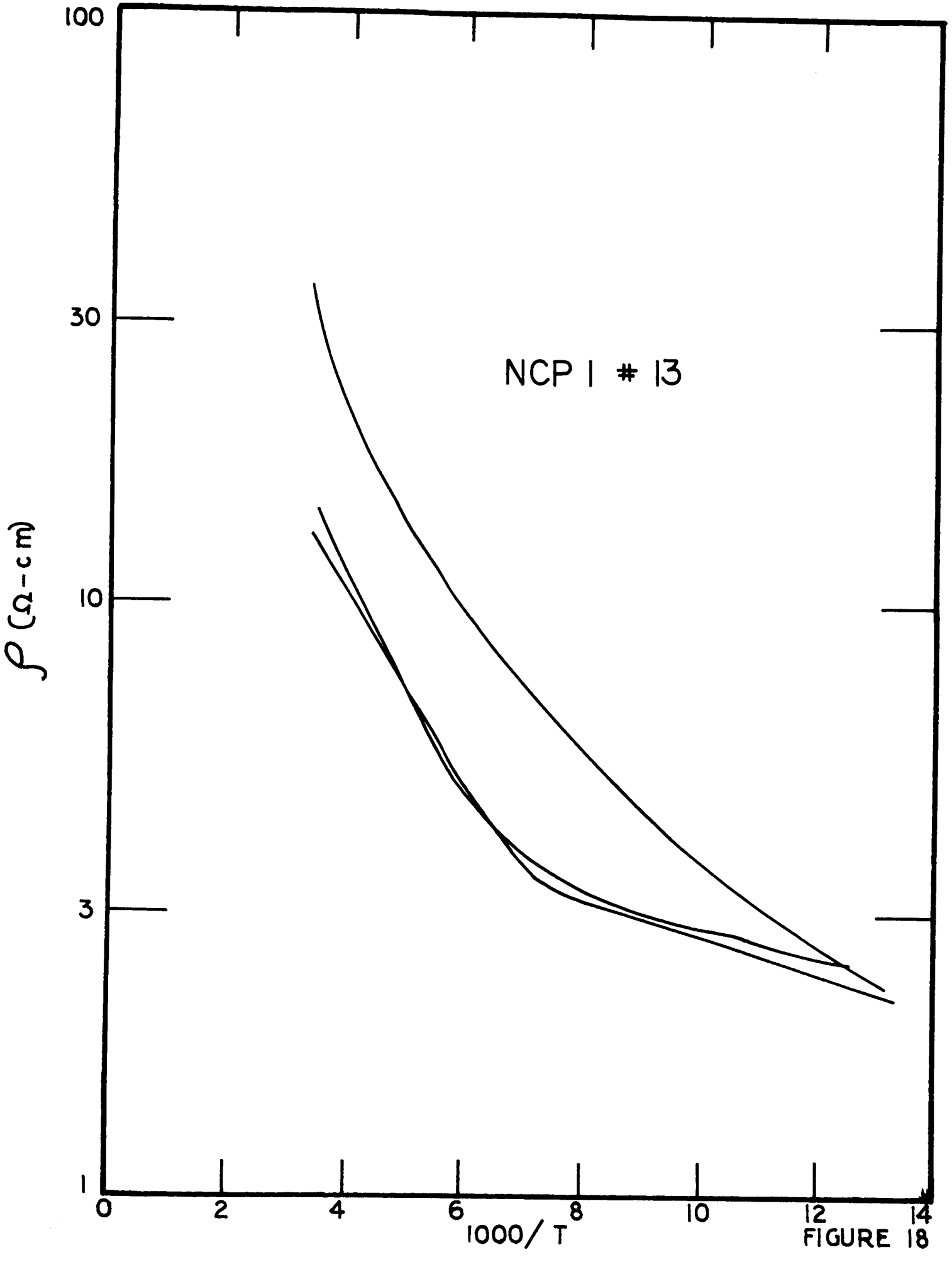

FIGURE 18

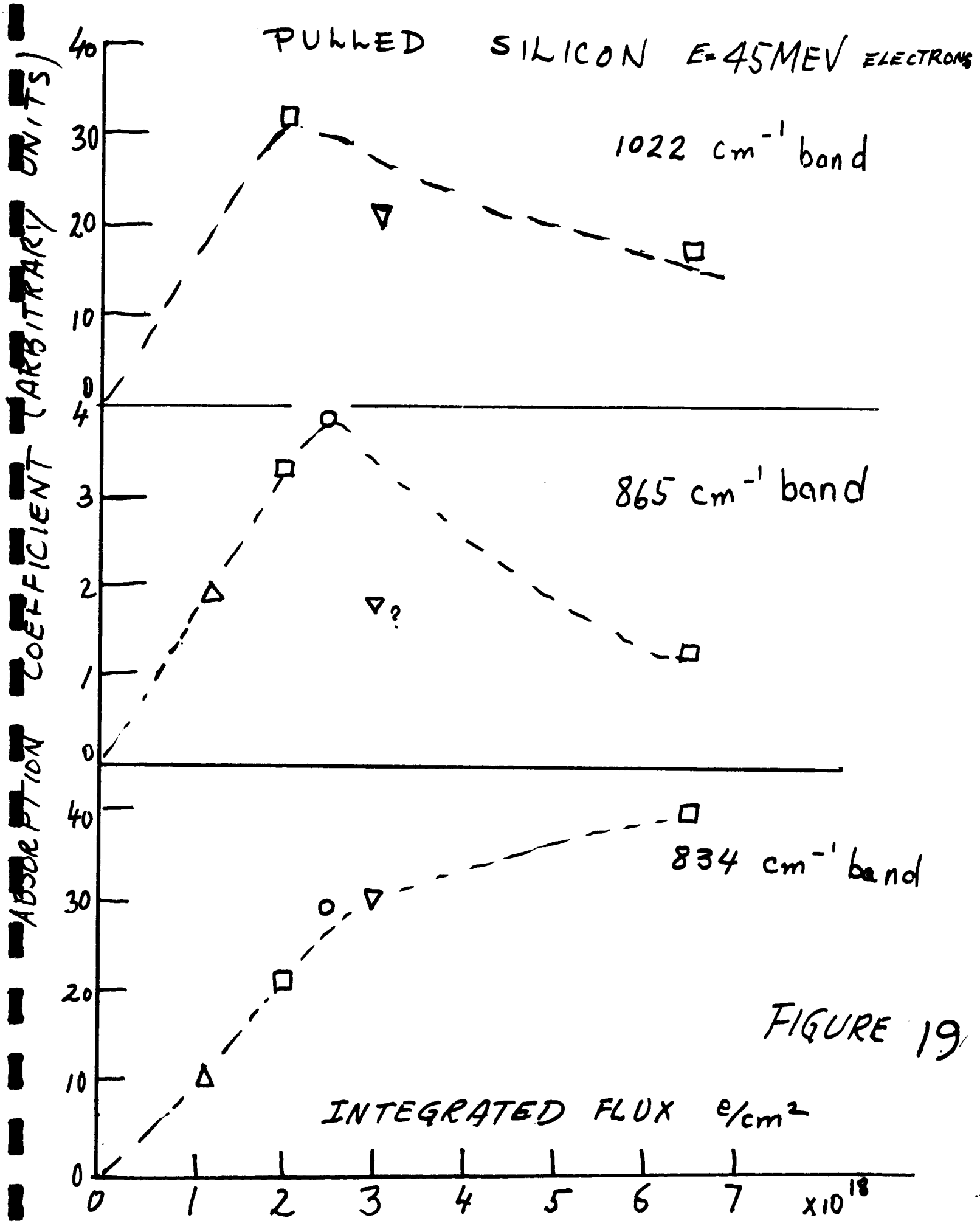
PULLED SILICON E=45MEV ELECTRONS
1022 cm⁻¹ band
865 cm⁻¹ band
834 cm⁻¹ band
ABSORPTION COEFFICIENT (ARBITRARY UNITS)
INTEGRATED FLUX e/cm²
x10¹⁸
0
1
2
3
4
5
6
7
10
20
30
40

FIGURE 19

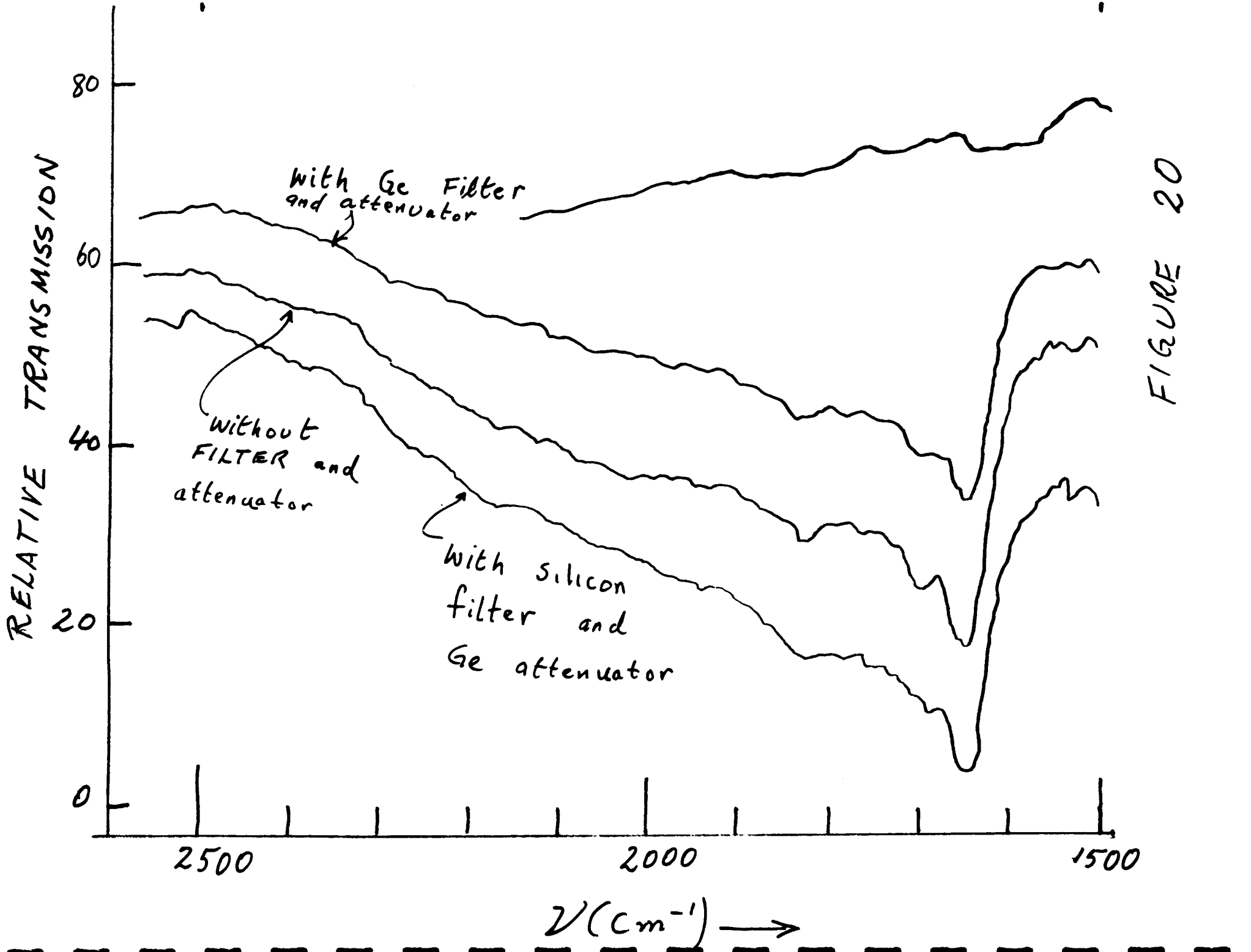
RELATIVE TRANSMISSION
80
60
40
20
0
With Ge Filter and attenuator
Without FILTER and attenuator
With silicon filter and Ge attenuator
2500
2000
1500
ν (cm⁻¹) →

FIGURE 20

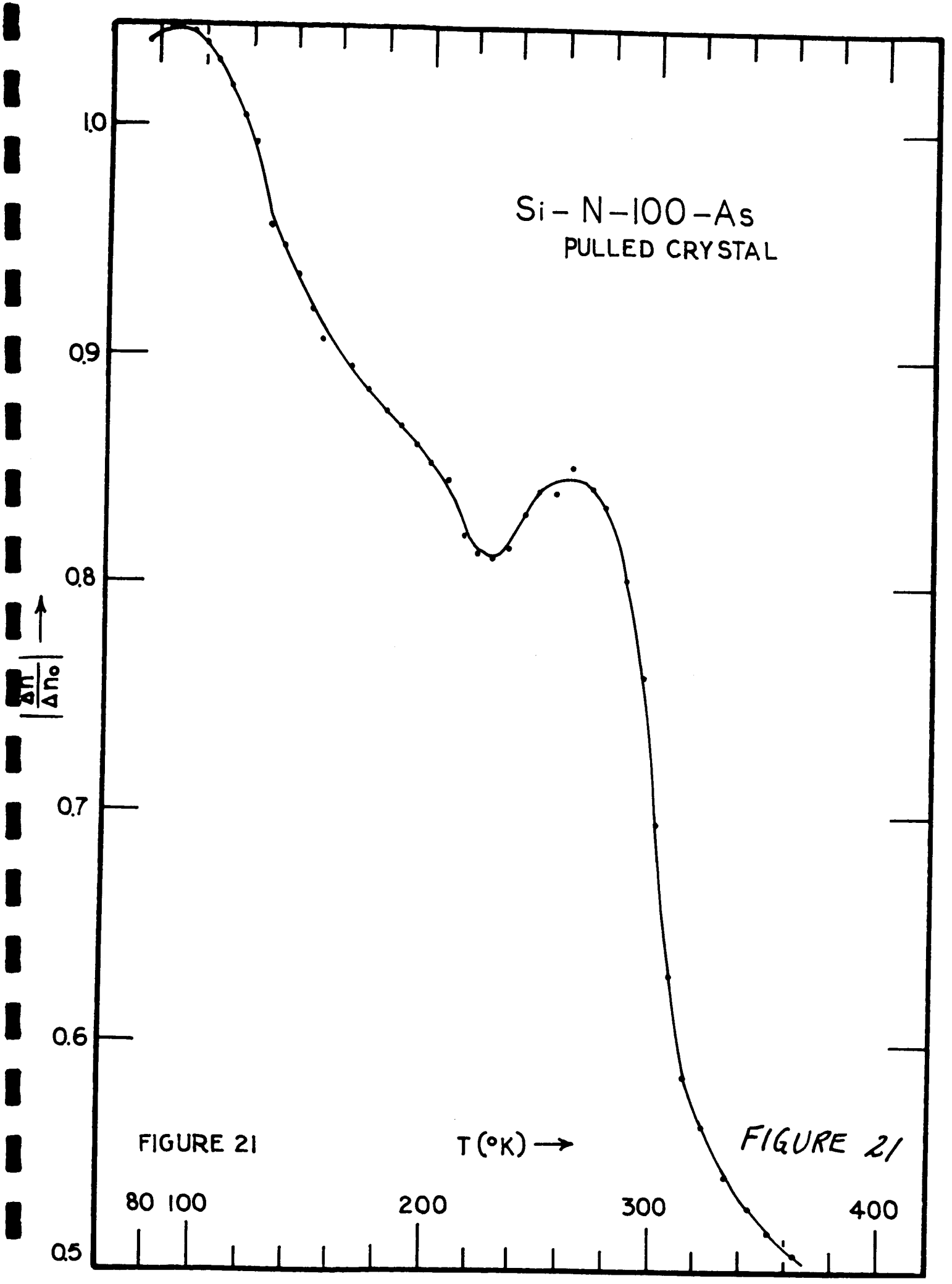

FIGURE 21

FIGURE 21

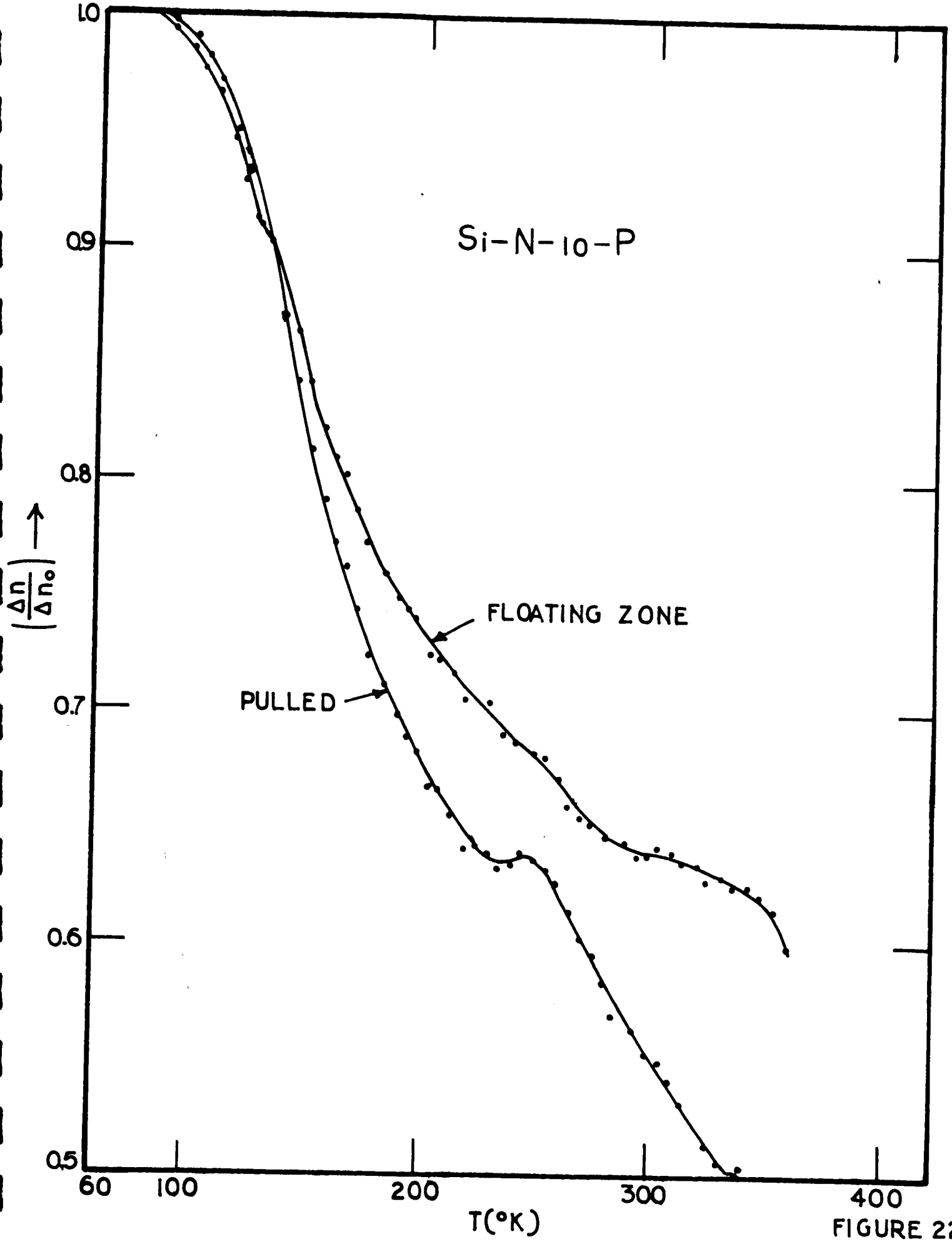
1.0
0.9
0.8
0.7
0.6
0.5
Si-N-10-P
FLOATING ZONE
PULLED
$\frac{\Delta n}{\Delta n_0}$
60
100
200
300
400
T(°K)

FIGURE 22

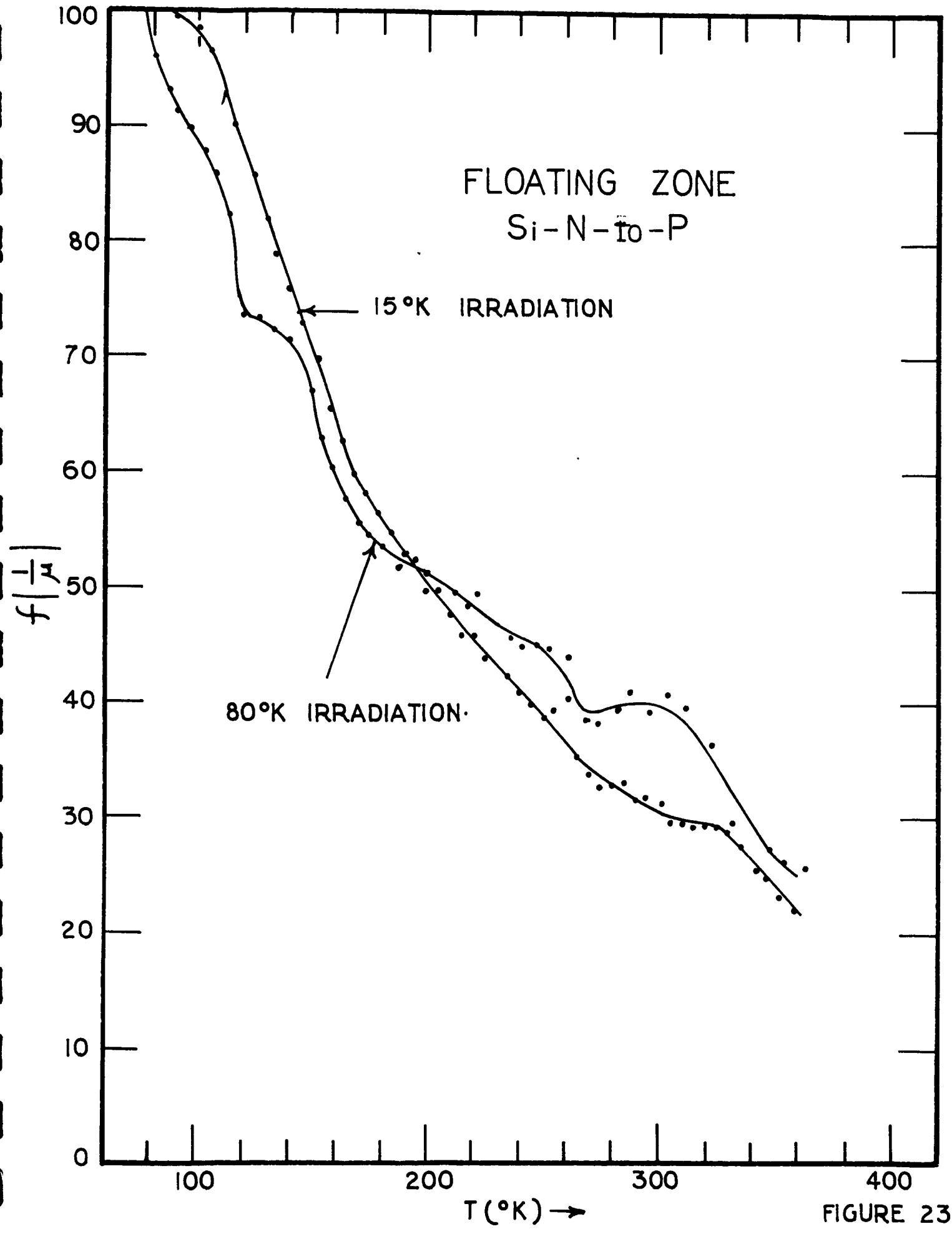
FLOATING ZONE
Si-N-To-P
15°K IRRADIATION
80°K IRRADIATION
100
90
80
70
60
50
40
30
20
10
0
100
200
300
400
T(°K) →

FIGURE 23

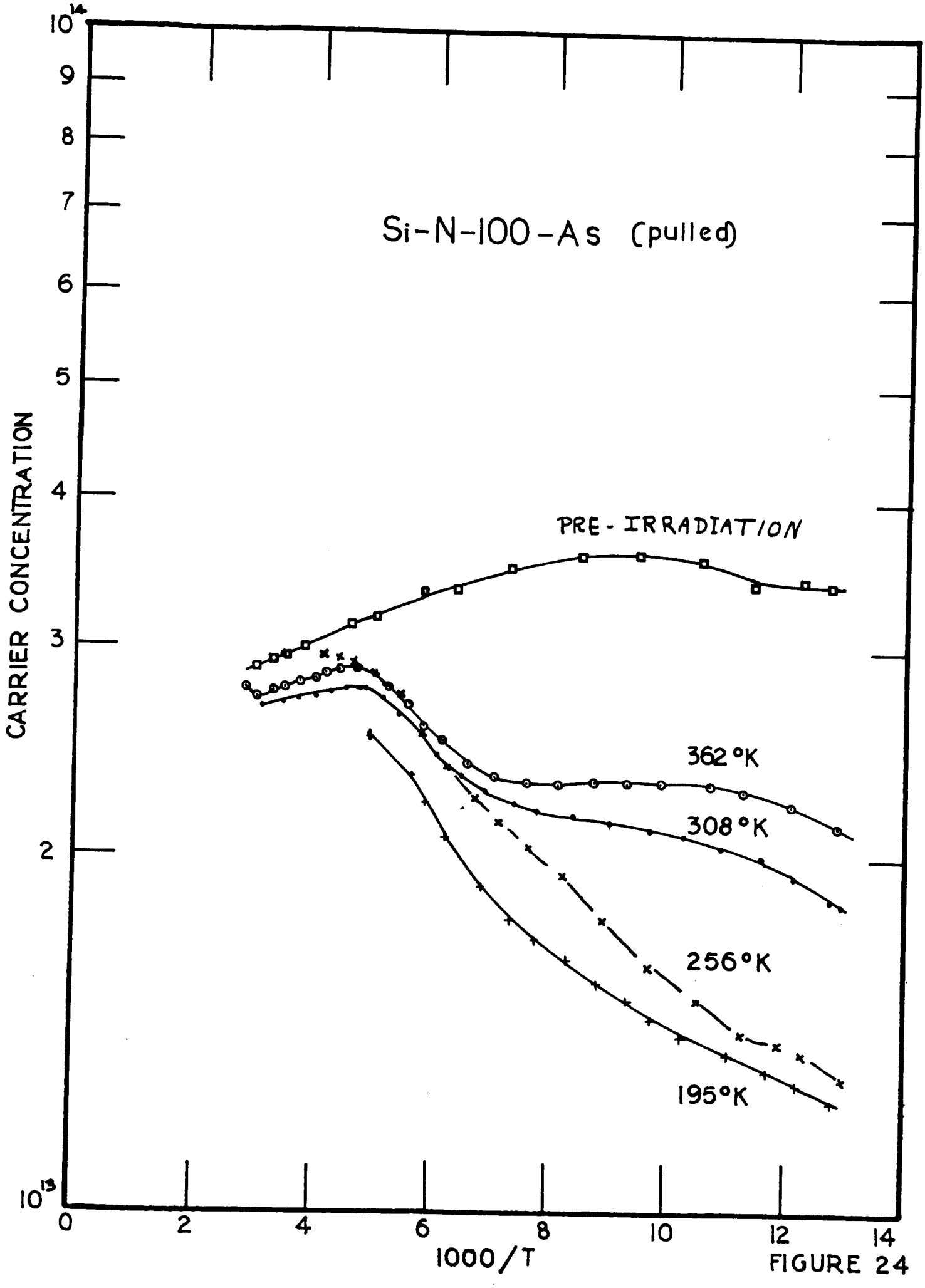
Si-N-100-As (pulled)
PRE-IRRADIATION
362°K
308°K
256°K
195°K
CARRIER CONCENTRATION
1000/T
10^{14}
9
8
7
6
5
4
3
2
10^{13}
0
2
4
6
8
10
12
14

FIGURE 24

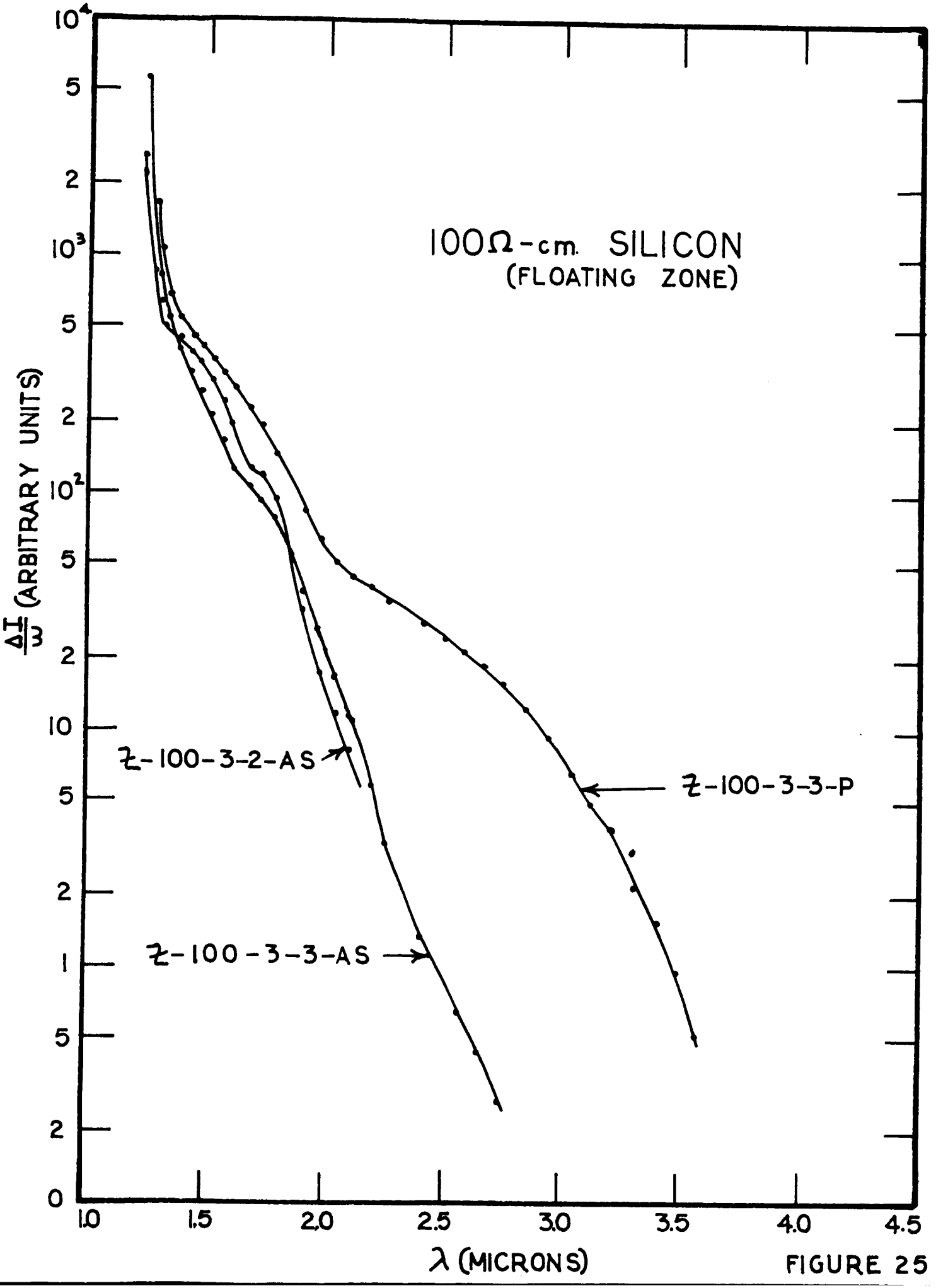
100Ω-cm. SILICON
(FLOATING ZONE)
$\frac{\Delta I}{3}$ (ARBITRARY UNITS)
λ (MICRONS)
Z-100-3-2-AS
Z-100-3-3-P
Z-100-3-3-AS
10^4
5
2
10^3
5
2
10^2
5
2
10
5
2
1
5
2
0
1.0
1.5
2.0
2.5
3.0
3.5
4.0
4.5

FIGURE 25